ERASMUS UNIVERSITY ROTTERDAM
Erasmus School of Economics

A Climate Risk Assessment of Eurozone Banks

Master Thesis Econometrics and Management Science
Quantitative Finance

Name student
Floor Louisa Raaijmakers
Student ID number
504680

Supervisor EUR
Prof. dr. PHBF Franses
Second Assessor EUR
B. van Os
Supervisor Triple A
M. Lamme

November 10, 2022

Abstract

Climate change risk is on top of the agenda for financial institutions. However, the far-reaching breadth of climate change risk combined with the intrinsic uncertainty makes the implications challenging to estimate. Our paper expands the work on CRISK by Jung, Engle and Berner (2021). CRISK measures the expected capital shortfall of a financial institution during a climate transition stress scenario. The risk metric uses a Climate Beta to measure the sensitivity of a bank to climate transition stress and proxies the stress scenario with a 'stranded asset' portfolio. The novelty of our research spans across two domains: first, we extend the scope and perform a Eurozone-focused analysis by shedding light on CRISK among 7 of the largest European banks. Moreover, we explore 3 climate stress severities and further the robustness by analyzing 3 different stranded assets. Second, we propose a novel methodology to calibrate the Climate Beta. We compute a non-parametric Climate Beta and introduce a new definition for CRISK in which the Climate Beta is a function of the climate stress severity. We follow the methodology of Maheu & Shamsi (2021) and use a non-parametric Dirichlet process mixture to estimate the posterior joint distribution of the bank and the stranded asset. Furthermore, we derive the Climate Beta according to the Dynamic Conditional Beta approach of Engle (2015). We compare our non-parametric multivariate GARCH model with a Dirichlet process prior to a parametric multivariate GARCH benchmark and find that our non-parametric model performs better in- and out-of-sample. The key insight of our paper is that the parametric model underestimates the Climate Beta during a climate transition stress event. Furthermore, although the non-parametric dynamic conditional Climate Beta allows for non-linear variation depending on the contemporaneous value of the stranded asset, we do not find supporting evidence for a non-linear response in the Climate Beta to the climate stress events studied. Lastly, while we find that CRISK increases during a climate transition stress event, we also find that most European banks are already experiencing high capital shortfall without climate stress conditioning and that the applied climate stress does not significantly change CRISK.

Keywords: climate finance, transition risk, systemic risk, stranded assets, CRISK, Climate Beta, non-parametric statistics, DCC, DCB, MGARCH, Dirichlet process mixture

Contents

1 Introduction

Climate change is one of the greatest challenges of the 21st century with potentially cataclysmic consequences for ecology and socio-economics. Due to the wide-ranging destabilizing effects, climate change introduces unprecedented uncertainty to financial risk. As a result, climate finance has proliferated in recent years and has regulators and practitioners reevaluating financial risk management. Climate change risk manifests in a myriad of ways, with the literature making the distinction between 'transition risk' and 'physical risk'. The former concerns the risks of transitioning to a low carbon economy and the latter the physical risks of a temperature increase above 1.5 degrees Celsius. Transition risk is expected to materialize faster relative to physical risk, and as physical risk is concerned with many geographical intricacies our paper will hereinafter focus on climate change risk from the perspective of transition risk.

The 2018 report of De Nederlandsche Bank (DNB) considers four scenarios of transition risk and identifies two catalysts: policy change and technological breakthrough (Vermeulen et al., 2018). Policy change is aimed at reducing carbon dioxide emissions, for example through a carbon tax. The report notes such a policy will increase the carbon price, but at the same time will induce economic slowdown and rising interest rates. A resemblance to this transition risk scenario was observed during the 2022 crisis in Ukraine. Furthermore, technological advancement in renewable energy will affect fossil fuel-intensive businesses, as a better alternative might replace the demand. DNB also considers a 'double shock scenario', where policy change and technological advancement occur simultaneously. Lastly, the report discusses a 'confidence shock' scenario, where the government fails to take action and consumer and investor confidence drops, resulting in higher risk premiums and lower consumption. In terms of scenario analysis, the Covid-19 crisis resembles the last scenario to an extent.

The vulnerability of financial institutions to transition risks is market and credit-based, yet mostly rooted in their credit exposure to transition-sensitive industries (Alogoskoufis et al., 2021). This vulnerability might be direct, for example, the creditworthiness of an oil manufacturer is directly affected when there is decreased demand due to decarbonization policy action. Or indirectly, where firms supporting the production of oil will be affected by their downturn, and thus might experience deterioration with respect to their default risk. In the Climate-Related Risk and Financial Stability Report, the European Systemic Risk Board (ESRB) predicts that the banking system losses could reach levels as high as 10% due to a credit rating fall for highly emitting firms under a carbon tax (ECB/ESRB, 2021). As systemic risk is known to be exacerbated in crisis scenarios and for its risk of reverberating through the real economy (Acharya et al., 2010) it is imperative to study the effects of transition risk on potential losses.

There is extensive discussion on how to weave transition risk into the existing risk framework. An example of such debate is the European Banking Authority's (EBA) final draft to develop

'implementing technical standards' (ITS) on Pillar 3 disclosures on environmental, social and governance (ESG) risks[1]. Pillar 3 refers to the Basel III Framework of the Basel Committee on Banking Supervision (BCBS), which is the global standard for prudential regulation of banks. The risk management proposal includes the request for elaborate disclosure on exposures towards carbon-intensive corporates as well as Taxonomy-aligned exposures. Moreover, the proposal includes the requirement for the implementation of ESG risk assessments in the form of stress tests and scenario analyses.

This discussion naturally gives rise to the quantification of transition risk during its decarbonization trajectory. Authors Jung, Engle and Berner (JEB) (2021) present the risk metric 'CRISK' which stands for the expected capital shortfall of a financial institution in a climate stress scenario. CRISK's predecessor is 'SRISK', which originated as a result of the adversity of failing institutions during the 2008 financial crisis (Brownlees & Engle, 2018). Whereas SRISK is conditioned on a systemic market crisis event, CRISK is conditioned on a systemic climate stress event. CRISK merges a firm's size, leverage and sensitivity to transition risk into a metric that can be compared to identify the most and least resilient institution when it comes to a systemic climate event. The central component to be calibrated in CRISK is the Climate Beta which measures the exposure of a financial institution to a Climate Factor. The Climate Beta mimics the sensitivity to a climate transition stress event and the Climate Factor is proxied by a 'stranded asset' portfolio (Jung et al., 2021) which is long in a 'stranded asset' and short in the market factor. A so-called 'stranded asset' refers to an asset that suffers from premature devaluation and in the context of climate change stress refers to assets such as oil and coal. Hence the stranded asset portfolio is expected to underperform as the economy progresses along its decarbonization trajectory. JEB estimate the Climate Beta according to Engle's Dynamic Conditional Beta (DCB) approach (2015) and adopt a multivariate normal distribution to model the joint returns of the financial institution and the Climate Factor.

Our paper adds to climate finance literature by expanding the work of JEB on CRISK. We apply a novel methodology to estimate the Climate Beta in CRISK by modeling the joint returns as a non-parametric infinite normal mixture model. This flexible density allows the Climate Beta to behave non-linearly conditional on the devaluation of the Climate Factor. This choice is motivated by the observation of JEB that there might be a non-linear relationship between the Climate Beta and the performance of the Climate Factor. We compare our non-parametric model to a parametric benchmark model to estimate the Climate Beta, where both estimation methods are variants of the DCB methodology. Our parametric benchmark models the joint returns as a multivariate Student-t distribution with a constant mean and conditional scale parameter. The conditional scale parameter is modeled by a multivariate GARCH process and this model is referred to as 'MGARCH-t'. We continue with modeling the joint returns as an infinite mixture of

[1] https://www.eba.europa.eu/eba-publishes-binding-standards-pillar-3-disclosures-esg-risks

multivariate normal distributions, where the mixing occurs over the mean and over the conditional covariance matrix. To infer the non-parametric mixture elements we use a Dirichlet process mixture and hence we refer to this model as 'MGARCH-DPM'. Using our non-parametric approach, we introduce a Climate Beta which is dynamic across both the dimension of time as well as the spectrum of contemporaneous values of the Climate Factor. Consequently, we also propose a new definition of CRISK which introduces a Climate Beta as a function of the climate stress severity.

In light of the EBA report, our research extends the scope of JEB's CRISK and performs a Eurozone-focused analysis to investigate the resilience of Eurozone banks to systemic climate change risk. As noted previously, hereby we give special attention to the estimation of the Climate Beta. Moreover, one of the novelties of our study is that we further the robustness of CRISK by assessing a range of climate stress scenarios and examining multiple Climate Factors. Furthermore, in the case of a non-parametric dynamic conditional beta, we investigate the potential non-linear response to a range of climate stress severities. Additionaly, a difference compared to JEB is that our paper will estimate the models through a Bayesian lens whereas JEB adopt a frequentist perspective. This bolsters our endeavor to approach the uncertainty of climate change risk with extra distribution and parameter precaution.

One of the key insights of our paper is that the MGARCH-DPM Climate Beta exhibits a stronger response to the climate transition stress event compared to the MGARCH-t estimated Climate Beta. We find that our MGARCH-DPM model performs better in- and out-of-sample from assessing the log-likelihood and predictive log-likelihood. Therefore, as our non-parametric model yields a higher likelihood, we deduce that the parametric benchmark underestimates the Climate Beta and therefore underestimates the effect on the capital shortfall. On the same note, we also deduce that the parametric benchmark model places too restrictive distributional assumptions on the joint density and fails to capture the dependence of a bank to a tail event in the Climate Factor. As tail risk is crucial in financial risk management, our finding supports our stand to approach the uncertainty of climate change risk with heightened distribution precaution. Another valuable insight of our research is that not all banks respond similarly to all Climate Factors. Thus, our paper stresses the inclusion of multiple Climate Factors to prevent a biased result for CRISK. Another important insight of our paper is that while the Climate Beta did exhibit differences across the banks in our analysis, the effect on CRISK was mostly insignificant. This raises the question to what extent CRISK clearly conveys the risks of climate transition risk as most of the banks are already experiencing high capital shortfalls without the conditioning of a hypothetical climate stress scenario.

The remainder of our paper proceeds as follows: Section 2 reviews the latest climate finance literature and places CRISK in the context of other climate risk adjusted metrics. This section further provides background on non-parametric statistics and the emergence of the Dirichlet

process prior. Section 3 outlines the methodology of the benchmark MGARCH-t model and our non-parametric MGARCH-DPM model. The Eurozone banks of choice and an overview of the data used to compute CRISK are outlined in Section 4. In Section 5 we present our empirical study and discuss the model configuration, model performance and the results for the Climate Beta and CRISK for both models. Finally, Section 6 discusses and concludes our main findings and proposes areas for future research.

2 Literature Review

Climate change risk is systemic by nature as its implications affect the entire financial system. The financial crisis of 2007-2009 revealed the devastating weaknesses of financial risk models. As a result, modeling systemic risk has since received exponential attention. The interlinkages between financial institutions are now well-known to amplify negative shocks (Battiston et al., 2017) and to result in negative externalities to the real economy in case of undercapitalization (Engle, 2018). Therefore, as noted by Engle (2018), it is important to perform scenario analysis on capital shortfall in systemic crisis events, as undercapitalized financial institutions are at heightened risk of negative shocks, and thereby prone to exacerbate a crisis. However, thus far, systemic crisis events are only based on the downturn of a market factor (Vinciguerra & Gaudemet, 2020). While financial institutions are expected by the Basel Framework to cover all market, credit and operational risks and therefore include the effect of climate change risk, in practice there is no common methodology to incorporate this to date.

Subsequently, climate change risk has received considerable attention and the integration is on top of the agenda for European supervisory institutions such as the EBA, the ESRB and the European Central Bank (ECB). In July 2021 the ECB and the ESRB published 'Climate-related risk and financial stability' (ECB/ESRB, 2021) and in September 2021 the ECB published an 'Economy Wide Climate Stress Test' (Alogoskoufis et al., 2021) which covers the climate risks for the wider economy. The ESRB uses a raised carbon price, from €20/tonne CO2 to €250/tonne CO2, to test the resilience of the banking system and find that the tail loss increases by 13% in a €100/tonne- and up to 40% in a €250/tonne scenario. One of the assumptions of the ESRB stress test is the homogeneous impact of carbon prices in relation to a firm's emissions. Contrarily, authors Huij et. al (2022) suggest a market-based 'carbon beta' which is the sensitivity of a stock to a 'pollutive-minus-clean' (PMC) factor. In their reasoning, the factor might capture a wider range of characteristics that measure climate risk exposure and does not assume the same sensitivity to a carbon price hike for stocks with equal emissions.

Similar to the PMC factor and to CRISK, literature has been expanding other financial risk models and metrics to incorporate climate risk. For example, Garnier et. al.'s Climate Extended Risk model (CERM) (2022) where the Basel Internal Ratings-Based (IRB) Asymptotic Single Risk Factor model (ASRF) is extended with systemic factors which account for physical and transition risk. Garnier introduces the concept of 'micro' and 'macro' sensitivities to systemic factors. The former is known as the obligor sensitivity to the macro economy factor in the ASRF model and the latter is a newly introduced parameter that models the evolution of the intensity of the systemic factor over time. Garnier experiments with varying evolutions of the 'macro' sensitivity to mimic different climate stress scenarios. In a similar fashion, Kenyon and Berrahoui (2021) introduce Climate Change Valuation Adjustment (CCVA) which measures the effect of including climate stress in the calculations of expected loss on counterparty default (Credit

Valuation Adjustment (CVA)) and the costs of funding (Funding Valuation Adjustment (FVA)). This is achieved by calibrating the time-dependent hazard rate in the general CVA and FVA formula on climate stress scenarios. Ojo-Ferreira, Reboredo, and Ugolini (2022) derive the CTER, CTVAR, and CTES, respectively the expected return, value-at-risk, and expected shortfall conditional on a climate transition stress scenario. The authors introduce a copula-based model which characterizes climate stress scenarios in terms of the co-movements of equity returns which either favor, 'green', or disfavor, 'brown', climate change. Consequently, the hedge properties of the financial institution to these movements grant insight into their climate change risk.

The currency of climate-adjusted metrics is evident and their novelty poses unique challenges to traditional risk analysis. In response, our paper consults a non-parametric method to analyze CRISK. Non-parametric statistics allow the data to infer the number of parameters in a model instead of confining them to a predefined set. As non-parametric statistics is often applied in uncertain circumstances it could prevent oversimplified distributional assumptions of a bank's sensitivity to a climate stress scenario. To account for the incertitude, we have modeled the joint returns as an infinite mixture of normal distributions using a Dirichlet process prior. Ferguson (1973) first proposed a Dirichlet process as a prior in non-parametric Bayesian analysis. As outlined in Ferguson, sampling from a Dirichlet process prior is similar to sampling a probability distribution from a set of probability distributions. It thus possesses the desirable property to span a large number of prior distributions. In addition, as the Dirichlet distribution is the conjugate prior to a multinomial distribution, the posterior distribution is analytically tractable. Escobar and West (1995) were the first to apply the Dirichlet process to estimate the non-parametric posterior density of a mixture of normals using Monte Carlo approximation. Their influential paper was driven by the advancement of Monte Carlo methods by Metropolis (1953), Hastings (1970) and Geman & Geman (1984) that allowed to numerically derive the complex posteriors. With our study, we aim to explore the possible advantages of non-parametric versus parametric Bayesian analysis and use the inferred Climate Beta and CRISK to gauge the resilience of Eurozone banks to climate stress.

3 Methodology

In this section, we outline the model components of CRISK for financial institutions of our choice. We first dissect the inputs of CRISK in Section 3.1. Continuing, we give an overview of Engle's Dynamic Conditional Beta method to derive the Climate Beta as required for CRISK and introduce our parametric MGARCH-t benchmark model with Dynamic Conditional Correlation MGARCH parametrization in Section 3.2. Moreover, in Section 3.3 we provide a detailed description of a Dirichlet Process Mixture and introduce our MGARCH-DPM model which models the joint returns as a non-parametric infinite normal mixture distribution.

3.1 CRISK

A financial institution experiences a capital shortfall (CS), when there is a positive difference between the required and the available capital. In case of a negative difference, we speak of a capital surplus. Financial institutions are obliged to hold prudential capital to safeguard them in times of downturn. The ECB published that for 2022 the capital requirements are 15.1% of a bank's Risk-Weighted-Assets (RWA)[2]. The RWA procedure assigns a percentage to different types of assets that a bank holds which is proportional to the level of riskiness as determined by the Supervisory Review and Evaluation Process (SREP). For CRISK, this is simplified to a capital fraction k which a financial institution is obliged to hold as required capital. JEB apply $k = 8\%$ in their paper.

$$\begin{aligned} CS &= k(ASSETS) - EQUITY \\ &= k(DEBT + EQUITY) - EQUITY \\ &= k \cdot DEBT - (1-k) \cdot EQUITY \end{aligned} \tag{1}$$

CRISK zooms into the expected capital shortfall conditional on a climate stress event. In this event, equity is expected to decline by the long-run-marginal expected shortfall (LRMES) as outlined in Engle (2018). In addition to the LRMES, CRISK consists of the market capitalization, $EQUITY$, and the debt book value, $DEBT$, of the financial institution. The LRMES is only applied to the bank's market capitalization as it is assumed that the value of debt does not change during a stress event.

$$\begin{aligned} CRISK &= (CS \mid \text{Climate Stress Event}) \\ &= k \cdot DEBT - (1-k) \cdot EQUITY \cdot (1 - LRMES) \end{aligned} \tag{2}$$

In order to calculate CRISK and LRMES one should define a Climate Factor which mimics a climate stress event. JEB use a 'stranded asset portfolio' as a proxy for climate transition risk, this portfolio is long in the stranded asset and short in the market portfolio. The stranded asset

[2] https://www.bankingsupervision.europa.eu/press/pr/date/2022

here refers to fossil fuels which are expected to suffer as a result of transition risk. JEB take the climate stress event as a 50% decrease, $\theta = 0.5$, in the stranded asset portfolio in 6 months.

In order to measure the effect of the climate stress event on the capital shortfall, JEB use a Climate Beta which measures the sensitivity of the bank's stock return, y, to the Climate Factor, x_{cf}, in a factor model which also includes a market factor, x_m, see Equation 3.

$$y_t = \beta_t^{Mkt} x_{m,t} + \beta_t^{Climate} x_{cf,t} + \epsilon_t \tag{3}$$

The LRMES derivation is depicted in Equations 4-6 as defined in Engle (2018).

$$\frac{p_{y,t+T}}{p_{y,t}} = \exp\left[\sum_{j=1}^{T}\left(\beta_{t+j}^{Mkt} x_{m,t+j} + \beta_{t+j}^{Climate} x_{cf,t+j} + \varepsilon_{t+j}\right)\right] \tag{4}$$

$$\frac{p_{y,t+T}}{p_{y,t}} \approx \exp\left\{\left(\beta_t^{Mkt}\right)\left[\log\left(\frac{p_{m,t+T}}{p_{m,t}}\right)\right] + \left(\beta_t^{Climate}\right)\left[\log\left(\frac{p_{cf,t+T}}{p_{cf,t}}\right)\right] + \sum_{j=1}^{T}\left(\varepsilon_{t+j}\right)\right\} \tag{5}$$

$$\text{LRMES} \equiv \text{Median}\left(\frac{p_{y,t} - p_{y,t+T}}{p_{y,t}} \mid \frac{p_{cf,t} - p_{cf,t+T}}{p_{cf,t}} = \theta\right) = 1 - \exp\left[\left(\beta_t^{Climate}\right)\log(1-\theta)\right] \tag{6}$$

Inserting the derivation of the LRMES into Equation 2 yields:

$$CRISK_t = k \cdot DEBT_t - (1-k) \cdot EQUITY_t \cdot \exp\left[(\beta_t^{Climate})\log(1-\theta))\right]. \tag{7}$$

As our focus is on the negative consequences on capital in a climate transition stress event we apply the addition of Marco and Jiron (2020) in Equation 8 to emphasize that we focus on a positive capital shortfall.

$$CRISK_t = max\left(0, k \cdot DEBT_t - (1-k) \cdot EQUITY_t \cdot \exp\left[(\beta_t^{Climate})\log(1-\theta))\right]\right) \tag{8}$$

Our addition to CRISK is that we allow the dynamic conditional Climate Beta to depend contemporaneously on the climate stress severity. Hereby the Climate Beta varies over time and is also a function of the climate stress event denoted by θ.

$$CRISK_t = max\left(0, k \cdot DEBT_t - (1-k) \cdot EQUITY_t \cdot \exp\left[(\beta_t^{Climate}(\theta)\log(1-\theta))\right]\right) \tag{9}$$

3.2 MGARCH-t

JEB apply a Climate Beta estimated by the Dynamic Conditional Beta (DCB) method (Engle, 2015). This method is used in the context of time-series regression analysis where the parameters can vary over time. Specifically, this method leverages heteroscedasticity and derives the beta conditional on the filtration. To showcase, we use our benchmark model which models the joint density returns following a multivariate Student-t distribution with constant mean μ, dynamic scale matrix H_t and degrees of freedom ν. Here r_t denotes the 3×1 dimensional vector of returns of the portfolio. The portfolio returns consist of the bank of choice, y, the market factor return, x_m, and the Climate Factor return, x_{cf}.

$$r_t \mid r_{1:t-1} \sim t(\mu, H_t, \nu), \tag{10}$$

$$H_t = \begin{bmatrix} H_{yy,t} & H_{yx_m,t} & H_{yx_{cf},t} \\ H_{x_m y,t} & H_{x_m x_m,t} & H_{x_m x_{cf},t} \\ H_{x_{cf} y,t} & H_{x_{cf} x_m,l} & H_{x_{cf} x_{cf},t} \end{bmatrix} \tag{11}$$

Hence the dynamic conditional Climate Beta is given by Equation 12.

$$\beta_t^{Climate} = H^{-1}_{x_{cf}x_{cf},t} H_{x_{cf}y,t} \tag{12}$$

However, in order to infer the dynamic conditional Climate Beta we require a process to model the dynamic scale parameter. The Generalized Auto-Regressive Conditional Heteroskedasticity (GARCH) model captures volatility clustering when modeling returns as proposed by Engle (1982) and Bollerslev (1986). The GARCH process models the volatility parameter as an Auto Regressive Moving Average (ARMA) type of process of the lagged- volatility and the observation. As we are looking at multiple return series we will perform a multivariate GARCH model (MGARCH). Estimating a multivariate GARCH model in a similar fashion as a univariate GARCH model can be arduous considering the large number of cross-correlations to take into account. In an answer to this, several parametrizations of the conditional correlations have been proposed including but not limited to VECH (Bollerslev, Engle, & Wooldridge, 1988), BEKK (Engle & Kroner, 1995), and the method we will use in our paper; Dynamic Conditional Correlation (DCC) (Engle, 2002).

The two-step DCC estimator decomposes the multivariate conditional covariance matrix as a product of the univariate GARCH processes and a dynamic conditional correlation matrix R_t.

$$H_t = D_t R_t D_t, \quad \text{where } D_t = \text{diag}\left\{\sqrt{h_{ii,t}}\right\} \tag{13}$$

The diagonal elements in matrix D_t contain the square root of the univariate conditional volatility

as estimated by a GARCH(1,1) model in Equation 14.

$$h_{ii,t} = \omega_{ii} + \alpha_{ii}\varepsilon^2_{i,t-1} + \beta_{ii}h_{ii,t-1} \tag{14}$$

$$D^2_t = \text{diag}\{\omega_{ii}\} + \text{diag} \odot \{\alpha_{ii}\}(y_t - \mu)(y_t - \mu)' + \text{diag}\{\beta_{ii}\} \odot D^2_{t-1} \tag{15}$$

The second step of the DCC parametrization is the estimation of correlation matrix $R_t = \{\rho_{ij,t}\}^N_{i,j=1}$. The diagonal elements of R_t correspond to the dynamic correlations. This matrix is deduced from process Q in Equation 16 where $\epsilon_t = y_t - \mu$, $z_t = D_t^{-1}\epsilon_t$ and $\overline{Q}$ equals the unconditional covariance.

$$Q_t = (1 - \gamma - \delta) \odot \overline{Q} + \gamma \odot z_{t-1}z'_{t-1} + \delta \odot Q_{t-1} \tag{16}$$

$$\rho_{ij,t} = \frac{q_{ij,t}}{\sqrt{q_{ii,t}}\sqrt{q_{jj,t}}}. \tag{17}$$

Stationarity conditions apply to both the H as well as the Q process. For the processes to be mean-reverting $\alpha_{ii} + \beta_{ii} < 1$ and $\delta + \gamma < 1$ (Engle, 2002).

3.3 MGARCH-DPM

The time-varying Climate Beta in the paper of JEB can attest to the importance of dynamic estimation of the Climate Beta. On the other hand, the authors note that the value of CRISK is often negative, and add that this is likely related to the non-linear relationship between the Climate Beta and the performance of fossil-fuel firms (Jung et al., 2021). Therefore suggesting that, while the betas are time-varying, the constancy of the beta fails to capture the true dependence of the Climate Factor and the bank's return. Maheu and Shamsi (MS) (2021) propose a non-parametric Bayesian approach to estimating the Dynamic Conditional Beta. In their paper, the authors elaborate that the constant relationship between the factors and the returns imposes a too restrictive assumption especially if the parametric distributional assumptions are not valid. This limitation could be alleviated by relaxing any restrictions made on the distribution. MS (2021) suggest a countably infinite mixture of normal distributions to jointly model financial returns.

$$r_t \mid W, \Theta \sim \sum_{j=1}^{\infty} \omega_j N\left(r_t \mid \Theta\right), \tag{18}$$

$$W = \{\omega_1, \omega_2, \dots\}, \omega_j > 0, \forall j, \tag{19}$$

$$\sum_{j=1}^{\infty} \omega_j = 1. \tag{20}$$

The beta is taken as the derivative of the contemporaneous conditional distribution of the returns

with respect to the factor return, as will be elaborated in Section 3.3.4. Thus, in the context of estimating the Climate Beta, this implies taking the derivative with respect to the Climate Factor.

3.3.1 Dirichlet Process Mixture

To infer the infinite normal mixture model we use a Dirichlet process mixture (DPM). A Dirichlet process is used to draw the mixing parameters and assign weights to the distribution components. The process is derived from the Dirichlet distribution, which is a K-dimensional generalization of the Beta distribution. Just like the Beta distribution, the Dirichlet distribution is defined on the interval [0,1] and is therefore useful for drawing probabilities. An additional property of the Dirichlet distribution is that all the realizations will add up to one. Hence, using a Dirichlet process to draw mixture weights is appropriate to ensure that the probability mass of the infinite mixture model adds up to 1.

Where the Beta distribution, Equation 21, takes two shape parameters, α and β, to define how the probability mass is divided over the probability space, the Dirichlet process takes a concentration parameter α and a base distribution G_0, see Equation 22. Drawing x_k realizations from a Dirichlet distribution is similar to drawing K times from a Beta distribution where the shape parameters would change depending on the previous realization. As this would lead to many different shape parameters, the so-called 'stick-breaking' representation of the Dirichlet process generalizes this process by continuously drawing from a $\text{Beta}(1, \alpha)$ distribution, where α corresponds to the concentration parameter as introduced by Ishwaran & James (2001).

$$x \sim \text{Beta}(\alpha, \beta), \alpha > 0, \beta > 0, x \in [0, 1] \tag{21}$$

$$G \sim \text{DP}(\alpha, G_0), \alpha > 0. \tag{22}$$

The 'stick-breaking' representation of the Dirichlet process is thought of as a stick of length 1 which can be continuously broken into smaller and smaller pieces. The portion that we break off is determined by a draw from the $\text{Beta}(1, \alpha)$ distribution. For example, if $v_1 \sim \text{Beta}(1, \alpha) = 0.4$, we break a 0.4 portion off the stick, and we continue breaking a part of the remaining 0.6 of the stick and repeat this K times. This process is represented by:

$$\omega_1 = v_1, \tag{23}$$

$$\omega_j = v_j \prod_{l=1}^{j-1} (1 - v_l), j > 1, \tag{24}$$

$$v_j \overset{iid}{\sim} \text{Beta}(1, \alpha). \tag{25}$$

The lengths of the sticks hereby map to the weights given to the individual normal components in the mixture model. Referring back to the Beta distribution, we can deduce what changing the

concentration parameter α for a Beta$(1, \alpha)$ would do: the higher the alpha, the higher is the probability of a small realization, thus the smaller chunks we break off the stick, and vice versa. As MS (2021) state, alpha can be thought of as the 'strength of belief' in base distribution G_0: "The larger α the more distinct elements will have non-negligible mass".

After the weights are drawn, the distribution G results from the summation of the product of the weights with their respective atoms, denoted in Equation 26 by θ. Atoms are the input parameters for each mixture component and are drawn from the base distribution G_0, in case of a normal kernel these atoms could be μ and σ^2. A draw from a Dirichlet process is therefore equivalent to drawing a probability distribution from a probability distribution:

$$\theta_1, \theta_2, ... \sim G_0, \tag{26}$$

$$G = \sum_{j=1}^{\infty} \omega_j \delta_{\theta_j}. \tag{27}$$

Where δ_{θ_j} denotes the Dirac delta function which is zero everywhere but has a mass point at θ_j. Merging this with Equation 18 gives the following distribution for return series r:

$$r_t \mid \Theta_t \sim N\left(r_t \mid \Theta_t\right), \tag{28}$$

$$\Theta_t \sim G, \tag{29}$$

$$G \mid \alpha, G_0 \sim DP(\alpha, G_0). \tag{30}$$

The unknown density of the returns in the case of a normal kernel is represented by :

$$f(r) = \int N\left(r \mid \Theta\right) p(\Theta \mid G) \mathrm{d}\Theta \tag{31}$$

$$G \sim DP(\alpha, G_0) \tag{32}$$

$$\Theta \equiv (\mu, \sigma^2) \tag{33}$$

3.3.2 Hierarchial Model

For our model, we estimate the distribution of returns according to an infinite normal mixture model. As described in the previous section, the DPM draws the mixing elements and determines the weights. For our infinite normal mixture model the mixing elements are μ_j and B_j, respectively over the mean and covariance matrix H_t. Hereby H_t follows an MGARCH process. Combining the mixing elements and the conditional covariance matrix, we retrieve the density of the returns as denoted in Equation 34.

$$p\left(r_t \mid \mu, B, W, H_t\right) = \sum_{j=1}^{\infty} \omega_j N\left(r_t \mid \mu_j, H_t^{1/2} B_j \left(H_t^{1/2}\right)'\right) \tag{34}$$

The hierarchical model of the MGARCH-DPM following Maheu & Shamsi (2021):

$$r_t \mid \phi_t, H_t \sim N\left(\xi_t, H_t^{1/2} \Lambda_t \left(H_t^{1/2}\right)'\right), t = 1, \ldots, T \tag{35}$$

$$\phi_t \equiv \{\xi_t, \Lambda_t\} \mid G \sim G, \tag{36}$$

$$G \mid \alpha, G_0 \sim DP\left(\alpha, G_0\right), \tag{37}$$

$$G_0 \equiv N\left(\mu_0, D\right) \times \mathcal{W}^{-1}\left(B_0, \nu_0\right). \tag{38}$$

Our paper deviates from MS with the selection for the MGARCH parametrization. Where MS apply a VECH parametrization, we adopt the DCC parametrization as used for our benchmark MGARCH-t model, for the full details see Section 3.2. As a Dirichlet process G is discrete, μ and B map to a set of unique points, while ξ_t and Λ_t denote draws from G. Due to G being a discrete probability distribution, it is possible to have repeated draws of μ_j and B_j.

3.3.3 Bayesian Inference

We infer the parameters in the hierarchical MGARCH-DPM model using Bayesian inference. This implies estimating the probability distribution of the unknown parameters given the data, known as the posterior distribution $p(\theta \mid x)$.

In order to deduce the posterior distribution, we apply Bayes' theorem in Equation 39. This theorem represents the posterior distribution as a function of the likelihood of the data given the parameters, $p(x \mid \theta)$, and our prior beliefs about the distribution of the parameters, $p(\theta)$. As $p(x)$ is a normalizing factor, we disregard the integral and continue with the product of the prior and likelihood in order to derive the proportional posterior distribution.

$$p(\theta \mid x) = \frac{p(x \mid \theta)p(\theta)}{p(x)} = \frac{p(x \mid \theta)p(\theta)}{\int p(x \mid \theta)p(\theta)d\theta} \tag{39}$$

$$\propto p(x \mid \theta)p(\theta) \tag{40}$$

The core difference between Bayesian inference and classical or frequentist estimation is that parameters are treated as probability distributions instead of fixed parameters. In the context of CRISK estimation, Bayesian inference might provide an advantage over classical estimation. Li, Clements and Drovandi (2021) endorse Bayesian inference on the GARCH parameters as the frequentist Maximum Likelihood estimation places Gaussian distributional assumptions on the parameters, whereas this might be different from the inferred posterior distribution.

We adopt a Monte Carlo Markov Chain (MCMC) sampling method to sample the posterior estimates of the parameters in Equations 35-38. Monte Carlo sampling involves drawing random samples and obtaining a numerical approximation. The Markov Chain addition implies that new samples are generated conditional on the previous sample. MCMC sampling knows various flavors and for our posterior inference, we apply Gibbs sampling (Geman & Geman, 1984; Gelfand & Smith, 1990). The Gibbs sampling algorithm (Equations 41-47) is initialized by assigning the observations to their initial cluster. In our case a cluster refers to a set of mixing elements, see Equation 36. After the initial assignment, we recursively re-assign every observation for M iterations to a new cluster based on the conditional distribution of the observation given the other observations. Here ϕ_t denotes the cluster parameters for observation r_t as shown in Equation 36.

$$\text{Initialize } \boldsymbol{\phi}_{1:T}^{(0)} = \left(\boldsymbol{\phi}_1^{(0)}, \ldots, \boldsymbol{\phi}_T^{(0)}\right) \tag{41}$$

$$\text{For } g = 1, 2, \ldots, M. \tag{42}$$

$$\boldsymbol{\phi}_1^{(g+1)} \sim \pi\left(\boldsymbol{\phi}_1 \mid \boldsymbol{\phi}_2^{(g)}, \boldsymbol{\phi}_3^{(g)}, \ldots, \boldsymbol{\phi}_T^{(g)}\right) \tag{43}$$

$$\boldsymbol{\phi}_2^{(g+1)} \sim \pi\left(\boldsymbol{\phi}_2 \mid \boldsymbol{\phi}_1^{(g+1)}, \boldsymbol{\phi}_3^{(g)}, \ldots, \boldsymbol{\phi}_T^{(g)}\right) \tag{44}$$

$$\vdots \tag{45}$$

$$\boldsymbol{\phi}_T^{(g+1)} \sim \pi\left(\boldsymbol{\phi}_T \mid \boldsymbol{\phi}_1^{(g+1)}, \ldots, \boldsymbol{\phi}_{T-1}^{(g+1)}\right) \tag{46}$$

$$\text{Return } \left\{\boldsymbol{\phi}_{1:T}^{(1)}, \boldsymbol{\phi}_{1:T}^{(2)}, \ldots, \boldsymbol{\phi}_{1:T}^{(M)}\right\} \tag{47}$$

We continue to execute a two-step estimation approach. The first step of every Gibbs iteration is the estimation of the posterior distribution of the mixing parameters $\Theta \equiv (\mu, B)$, and the second step is the estimation of the conditional posterior distribution of the GARCH parameters which is conditional on the sampled Θ parameters in step one.

The striking characteristic of modeling the infinite normal mixture model in Equation 34 with a Dirichlet process lies in its ability to discover new clusters of mixing parameters depending on the data instead of categorizing data among a predefined set of clusters. However, in practice, it is impossible to sample and store an infinite amount of mixing components as displayed in Equation 27. Applying the logic that a component of the infinite normal mixture distribution only ever evolves to a cluster when an observation is assigned to a particular component (only if $N \to \infty$ we

discover all clusters), we can circumvent the need to draw an infinite amount of initial components. Several methods exist in the literature: Walker (2007) introduces 'slice sampling' which draws a uniformly distributed latent variable to decide where to truncate the component sampling. Papaspiliopoulos and Roberts (2008) circumvent this by 'retrospective sampling' and also introduce a latent uniformly distributed variable that dictates where on 'the stick' (referring to the stick-breaking representation of the Dirichlet process) the observation is sampled from. As noted in the previous section, the different lengths of the unit stick represent the chances of an observation falling into a specific cluster. Therefore, using a draw from a uniform variable Papaspiliopoulos and Roberts indirectly cover the infinite number of distribution components whose probabilities sum up to 1. In our paper, we apply Neal's algorithm 8 (2000) also known as a 'Chinese Restaurant Process' (CRP), which is a clustering method where an observation is clustered proportional to the number of observations in a cluster and can also discover a new cluster infinitely many times should that be necessary.

As noted in Equations 41-47, the Gibbs sampling method is initialized by assigning all observations to the 'first' cluster (the cluster labels are arbitrary), for which we draw its cluster parameters ϕ_c from G_0. We iterate over all observations and assign them either to the existing cluster or to a new cluster. This decision is dictated by the CRP and we continue by making a categorical draw according to the probabilities in Equation 48. The observations are labeled as $t = 1 \dots T$ and have corresponding cluster labels $c = (c_1, \dots, c_T)$ with cluster parameters $\phi = (\phi_c : c \in \{c_1, \dots, c_T\})$. We denote k^- as the number of distinct clusters and set $h = k^- + m$ where m is an integer of choice and controls how many new clusters are considered. For every observation, we first verify if removing the observation from its current cluster would leave the cluster empty. Should this be the case for observation t, c_t received label $k^- + 1$, and we draw new atoms for ϕ_c for which $k^- + 1 < c \leq h$. If after the removal of observation i the cluster is not empty, we draw new values for ϕ_c from G_0 for $k^- < c \leq h$.

We see in Equation 48 how an observation is assigned to an existing cluster proportional to the number of observations existing in the cluster, $n_{-t,c}$, times the likelihood of the observation in question to belong to that cluster. Furthermore, an observation might also 'discover' a new cluster with a probability proportional to the likelihood of an independently drawn atom from base measure G_0 times the concentration parameter α.

$$P\left(c_t = c \mid c_{-t}, r_t, \phi_1, \dots, \phi_h\right) \propto \begin{cases} n_{-t,c} N\left(r_t, \mid \phi_c\right) & \text{for } 1 \leq c \leq k^- \\ \frac{\alpha}{m} N\left(r_t, \mid \phi_c\right) & \text{for } k^- < c \leq h \end{cases} \tag{48}$$

After every observation has been assigned a new cluster we remove all the clusters with no members. We update the cluster parameters at the end of every iteration by computing the posterior estimate based on the observations that have been assigned to each cluster. The

configuration set that partitions the data $r_{1:T}$ into k^- unique clusters is denoted by $s_{1:T} = (s_1, \ldots, s_T)$ (Maheu & Shamsi, 2021).

In order to sample the posterior cluster parameters, we apply the results of conditional conjugate priors of the multivariate normal likelihood distribution. Conjugate priors imply that the posterior estimate is analytically tractable. However, in our case, the posterior estimates depend on one another and hence they are called conditionally conjugate. The posterior parameters of mixing elements μ and B follow:

$$B_j \mid r_{1:T}, s_{1:T}, \mu_j, \Gamma \sim \mathcal{W}^{-1}\left(n_j + \nu_0, B_0 + \sum_{s_t=j}\left(z_t - H_t^{-1/2}\mu_j\right)\left(z_t - H_t^{-1/2}\mu_j\right)'\right), \tag{49}$$

$$\mu_j \mid r_{1:T}, s_{1:T}, B_j, \Gamma \sim N(\bar{\mu}, \bar{D}), \tag{50}$$

in which (51)

$$\bar{D}^{-1} = D^{-1} + \sum_{t|s_{t=j}} H_t^{-1/2'} B_j^{-1} I_t^{-1/2}, \bar{\mu} = \bar{D}\left(\sum_{t|s_t=j} H_t^{-1/2'} B_j^{-1} z_t + D^{-1}\mu_0\right). \tag{52}$$

Where z_t is equal to $H_t^{-1/2} r_t$, and $\mathcal{W}^{-1}$ denotes the inverse Wishart distribution, see the Appendix for distributional details.

Due to the conditional conjugacy, we apply a Metropolis-Hastings (1970; 1953) step to sample the new parameters. This is achieved by iteratively sampling a new posterior parameter for B_j which is used as input for posterior μ_j, which is in the next Metropolis-Hastings iteration used as input for the posterior B_j again and so forth. The Metropolis-Hastings algorithm belongs to the MCMC family of sampling methods and introduces the concept of an acceptance criterion of the new sample: the new sample is accepted with a probability proportional to Equation 53. Hence if the sample sufficiently improves the posterior probability of the parameters given the data the chances increase that the new parameter sample is accepted.

$$\min\left\{\frac{N\left(r \mid \Theta^{i+1}\right) p\left(\Theta^{i+1}\right)}{N\left(r \mid \Theta^{i}\right) p\left(\Theta^{i}\right)}, 1\right\} \tag{53}$$

After this, we update the concentration parameter α. Similar to MS (2021), we follow West (1992) and impose a gamma prior on α, $\alpha \sim \mathcal{G}(a_0, b_0)$. We have previously defined k^- as the number of unique clusters discovered by the data and using this posterior information we proceed to update α by a two-step sampling method. This approach, as depicted in Equations 54-56, introduces auxiliary variable τ and draws a new α from a mixed gamma distribution with probabilities π_τ

and $1 - \pi_\tau$.

$$(\tau \mid \alpha, k^-) \sim \text{Beta}(\alpha + 1, T) \tag{54}$$

$$\alpha \mid \tau \sim \pi_\tau \mathcal{G}\left(a_0 + k^-, b_0 - \log(\tau)\right) + (1 - \pi_\tau)\, \mathcal{G}\left(a_0 + k^- - 1, b_0 - \log(\tau)\right) \tag{55}$$

$$\text{where } \pi_\tau = \frac{\pi_\tau}{1 - \pi_\tau} = \frac{a_0 + k^- - 1}{T\,(b_0 - \log(\tau))} \tag{56}$$

The first step of the posterior inference entails updating the posterior estimates of the mixing parameters and the concentration parameter α. Using this information we continue to the second step of the posterior inference and update the MGARCH parameters $\Gamma = (\omega, \alpha, \beta, \lambda, \delta)$. The posterior estimate of the MGARCH parameters, Γ, conditional on the mixing parameters,Θ, is given by:

$$p\left(\Gamma \mid \Theta, s_{1:T}, r_{1:T}\right) \propto p(\Gamma) \times \prod_{t=1}^{T} N\left(r_t \mid \mu_{st}, H_t^{1/2} B_{st} \left(H_t^{1/2}\right)'\right). \tag{57}$$

3.3.4 Non-Parametric Dynamic Conditional Beta

In the previous section, we outlined how we estimate the infinite normal mixture model defined in Equation 73 with a DPM. Using the CRP we sampled a finite $K^{(g)}$ clusters for every $g = 1, \ldots, M$ iteration which estimates the posterior distribution of the joint returns.

Using the posterior distribution we extract the Climate Beta by taking the derivative of the expected value of the conditional distribution of each cluster with respect to the Climate Factor and weigh this by the probability of the observation belonging to the said cluster.

This result follows from the conditional normal lemma given by:

$$y_t \mid x_t \sim N\left(\mu_{y|x}, H_{t,y|x}\right) \tag{58}$$

$$\mu_{y|x} = \mu_y + H_{yx,t} H_{xx,t}^{-1}\left(x_t - \mu_x\right) \tag{59}$$

$$H_{t,y|x} = H_{yy,t} - H_{yx,t} H_{xx,t}^{-1} H_{yx,t}' \tag{60}$$

The non-parametric Climate Beta is therefore given by:

$$\beta_t^{Climate}\left(x_{cf,t}\right) = \frac{\partial E\left(y_t \mid x_{m,t}, x_{cf,t}, r_{1:T}\right)}{\partial x_{cf,t}}. \tag{61}$$

Hereby the cluster-specific Climate Beta is defined as:

$$\beta_t^{Climate,(M)} = \frac{\left(H_t^{(M)^{1/2}} B_{s_t} H_t^{(M)^{1/2'}}\right)_{13}}{\left(H_t^{(M)^{1/2}} B_{s_t} H_t^{(M)^{1/2'}}\right)_{33}}. \tag{62}$$

We use Bayes' theorem to derive the conditional posterior distribution, which is denoted by:

$$p\left(y_t \mid \mathbf{x}_t, r_{1:T}, G^{(M)}\right) = \frac{p\left(y_t, \mathbf{x}_t \mid r_{1:T}, G^{(M)}\right)}{p\left(\mathbf{x}_t \mid r_{1:T}, G^{(M)}\right)}. \tag{63}$$

Hence, we require the joint distribution of the returns and the marginal distribution of the factor returns. The joint density of the returns $r_t = (y_t, \mathbf{x_t})$ and the factors $\mathbf{x_t} = (x_{m,t}, x_{cf,t})$ conditional on $G^{(M)}$ are given by :

$$p\left(y_t, \mathbf{x}_t \mid r_{1:T}, G^{(M)}\right) = \sum_{j=1}^{K^{(M)}} \omega_j^{(M)} N\left(y_t, \mathbf{x}_t \mid \theta_j^{(M)}\right). \tag{64}$$

Recalling that for iteration g a draw from a Dirichlet process is given by:

$$G^{(g)} = \sum_{j=1}^{K^{(g)}} \omega_j^{(g)} \delta_{\theta_j^{(g)}}. \tag{65}$$

The marginal distribution of the factors is given by Equation 66 and refers to the partition of the joint density in Equation 64.

$$p\left(\mathbf{x}_t \mid r_{1:T}, G^{(M)}\right) = \sum_{j=1}^{K^{(M)}} \omega_j^{(M)} N_{23}\left(\mathbf{x}_t \mid \theta_j^{(M)}\right) \tag{66}$$

Hence, inserting the results from Equation 64 and 66 into Equation 63:

$$p\left(y_t \mid \mathbf{x}_t, r_{1:T}, G^{(M)}\right) = \frac{\sum_{j=1}^{K^{(M)}} \omega_j^{(M)} N\left(y_t, \mathbf{x}_t \mid \theta_j^{(M)}\right)}{\sum_{j=1}^{K^{(M)}} \omega_j^{(M)} N_{23}\left(\mathbf{x}_t \mid \theta_j^{(M)}\right)}. \tag{67}$$

$$= \sum_{j=1}^{K^{(M)}} q_j^{(M)}(\mathbf{x}_t) N\left(y_t \mid \mathbf{x}_t, \theta_j^{(M)}\right) \tag{68}$$

Where the function q defines the weights given to each cluster and is defined by:

$$q_j^{(M)}\left(\mathbf{x}_t\right) = \frac{\omega_j^{(M)} N_{23}\left(\mathbf{x}_t \mid \theta_j^{(M)}\right)}{\sum_{j=1}^{K^{(M)}} \omega_j^{(M)} N_{23}\left(\mathbf{x}_t \mid \theta_j^{(M)}\right)} \tag{69}$$

As a result, the expected value of the conditional distribution following the lemma in Equation 59 is denoted by:

$$E\left(y_t \mid \mathbf{x}_t, r_{1:T}, G^{(M)}\right) = \sum_{j=1}^{K^{(M)}} q_j^{(M)}\left(\mathbf{x}_t\right)\left[\mu_{j,y}^{(M)} + \begin{bmatrix} \beta_{jt}^{Mkt,(M)} \\ \beta_{jt}^{Climate,(M)} \end{bmatrix}' \left(\begin{bmatrix} x_{m,t} \\ x_{cf,t} \end{bmatrix} - \begin{bmatrix} \mu_{j,m}^{(M)} \\ \mu_{j,cf}^{(M)} \end{bmatrix}\right)\right] \tag{70}$$

We continue by taking the derivative of the previous expression with respect to the Climate Factor. Applying the chain rule we retrieve the following expression:

$$\begin{aligned} \frac{\partial E\left(y_t \mid \mathbf{x}_t, r_{1:T}, G^{(M)}\right)}{\partial x_{cf,t}} = & \sum_{j=1}^{K^{(M)}} \left[\frac{\partial}{\partial x_{cf,t}} q_j^{(M)}\left(\mathbf{x}_t\right)\right]\left[\mu_{j,y}^{(M)} + \begin{bmatrix} \beta_{jt}^{Mkt,(M)} \\ \beta_{jt}^{Climate,(M)} \end{bmatrix}' \left(\begin{bmatrix} x_{m,t} \\ x_{cf,t} \end{bmatrix} - \begin{bmatrix} \mu_{j,m}^{(M)} \\ \mu_{j,cf}^{(M)} \end{bmatrix}\right)\right] \\ & + \beta_{jt}^{Climate,(M)} q_j^{(M)}\left(\mathbf{x}_t\right) \end{aligned} \tag{71}$$

Where the partial derivative of function q with respect to the return of the Climate Factor is derived using the quotient rule and applying the result of the derivative of a logarithmic function.

$$\begin{aligned} \frac{\partial}{\partial x_{cf,t}} q_j^{(M)}\left(\mathbf{x}_t\right) = & \frac{\left[\sum_{j=1}^{K^{(M)}} \omega_j^{(M)} N_{23}\left(\mathbf{x}_t \mid \theta_j^{(M)}\right)\right]\left[\frac{\partial}{\partial x_{cf,t}} \omega_j^{(M)} N_{23}\left(\mathbf{x}_t \mid \theta_j^{(M)}\right)\right]}{\left[\sum_{j=1}^{K^{(M)}} \omega_j^{(M)} N_{23}\left(\mathbf{x}_t \mid \theta_j^{(M)}\right)\right]^2} \\ & - \frac{\left[\frac{\partial}{\partial x_{cf,t}} \sum_{j=1}^{K^{(M)}} \omega_j^{(M)} N_{23}\left(\mathbf{x}_t \mid \theta_j^{(M)}\right)\right]\left[\omega_j^{(M)} N_{23}\left(\mathbf{x}_t \mid \theta_j^{(M)}\right)\right]}{\left[\sum_{j=1}^{K^{(M)}} \omega_j^{(M)} N_{23}\left(\mathbf{x}_t \mid \theta_j^{(M)}\right)\right]^2} \end{aligned} \tag{72}$$

To derive the derivative of the multivariate normal distribution with respect to the return of the Climate Factor we took the derivative of the log of the multivariate normal distribution and used the rule that the logarithmic derivative of a function is the derivative of the function divided by the function itself.

4 Data

4.1 Data Collection

Our research concerns Eurozone banks, more specifically, banks under the supervision of the ECB[3] per 1st of July 2022, who operate with a minimum size of 100 billion Euros and whose shares are traded publicly. We refer to the banks by their name and corporation status as stated by the ECB. Table 1 summarizes the selection of banks and the summary statistics can be found in Table 3.

	Country	**Ticker**	**Size**
Banco Santander, S.A.	Spain	SAN SM	EUR 1,000 bn+
Bank of Ireland Group plc	Ireland	BIRG LON	EUR 100-150 bn
BNP Paribas S.A.	France	BNP FP	EUR 1,000 bn+
Deutsche Bank AG	Germany	DBK GR	EUR 1,000 bn+
Erste Group Bank AG	Austria	EBS AV	EUR 150-300 bn
ING Groep N.V.	the Netherlands	INGA NA	EUR 500-1000 bn
Intesa Sanpaolo S.p.A	Italy	ISP IM	EUR 500-1000 bn

Table 1: Selection of Eurozone Banks.

To compute CRISK for the financial institution of choice we require data for the equity price, the market capitalization, and the book value of debt. We retrieve the book value of debt from Compustat - Capital IQ via Wharton Research Data Services (WRDS). The data is sourced from the Global section under 'Fundamentals Quarterly' and using query variable `LTQ -- Liabilities - Total (LTW)`. The market capitalization is computed by multiplying the equity price by the number of shares outstanding. Both the equity price and the number of shares outstanding are sourced from Bloomberg with query variables `px_last` and `eqy_sh_out` respectively.

In order to calibrate the Climate Betas, we form portfolios consisting of three stocks: the bank of choice, a market factor that proxies the market return, and a Climate Factor that proxies the climate transition stress event. The Climate Factor is short in the market and long in the stranded asset. For the former we selected the STOXX Europe 600 for the market return and for the latter we chose the iShares STOXX Europe 600 Oil & Gas UCITS ETF DE, the Lyxor STOXX Europe 600 Oil & Gas UCITS ETF, and the Invesco STOXX Europe 600 Optimised Oil & Gas UCITS ETF Acc as stranded assets. These Exchange Traded Funds (ETF) were selected due to their liquidity and diversified exposure to Eurozone-stranded assets. A summary is depicted in Table 2.

[3] https://www.bankingsupervision.europa.eu/banking/list

	Ticker	AUM	Inception
iShares STOXX Europe 600 Oil & Gas	SXEPEX GR	EUR 986.373.5m	8th Jul 2002
Lyxor STOXX Europe 600 Oil & Gas	OIL FP	EUR 13,386.1m	25th Oct 2006
Invesco STOXX Europe 600 Oil & Gas	XEPS GY	EUR 14,043.7m	7th Jul 2009

Table 2: Selection of Stranded Assets. AUM refers to Assets Under Management.

We use daily stock return data and our estimation period spans from the 1st of January 2010 to the 1st of August 2022. The summary statistics of all the indices are displayed in Table 3 below.

	Mean	Variance	Skewness	Kurtosis	Max	Min
Bank						
Banco Santander, S.A.	-0.016	5.026	0.203	10.119	23.218	-19.885
Bank of Ireland Group plc.	0.009	11.239	0.048	6.070	23.076	-23.256
BNP Paribas S.A.	0.024	5.349	0.312	8.412	20.897	-17.400
Deutsche Bank AG	-0.013	5.792	0.127	4.112	14.327	-15.881
Erste Group Bank AG	0.031	5.545	-0.072	5.269	15.178	-16.409
ING Groep N.V.	0.041	5.889	0.245	9.610	24.587	-19.372
Intesa Sanpaolo S.p.A	0.019	6.179	-0.261	7.362	19.678	-22.941
Market						
STOXX Europe 600	0.022	1.153	-0.620	8.894	8.405	-11.478
Stranded Asset						
iShares Europe 600 Oil & Gas	0.022	1.153	-0.620	8.894	8.405	-11.478
Lyxor Europe 600 Oil & Gas	0.024	2.260	-0.472	12.104	13.541	-16.771
Invesco Europe 600 Oil & Gas	0.026	2.238	-0.444	13.396	15.308	-17.268
Climate Factor						
OIL - SXXP	0.001	0.916	0.077	8.153	6.537	-9.328
SXEPEX - SXXP	-0.010	1.296	0.220	13.663	9.422	-9.688
XEPS - SXXP	0.004	0.894	0.080	8.961	6.903	-9.825

Table 3: Descriptive statistics of the daily returns from the 1st of January 2010 to the 1st of August 2022 of the banks of choice, the market factor, the stranded asset and the Climate Factor.

4.2 Data Processing

The daily price data of the indices is transformed to return data applying Equation 73.

$$r_t = \frac{p_t - p_{t-1}}{p_{t-1}} \times 100 \tag{73}$$

While forming the portfolios it could occur that a particular index did not share a trading day with the other indices due to, for example, a public holiday. For missing return data, we interpolated the price data point over the number of missing trading days.

As noted above, we are using daily return data and will analyze a daily CRISK. In this pursuit, we have chosen to interpolate the liabilities as well as the number of shared outstanding, as this data is reported quarterly or semi-annually. In case of missing data, we have applied a similar method as described above.

5 Empirical Results

The results presented in this section have been computed by the Dutch National Supercomputer Snellius[4]. Snellius is a batch system running on Linux and is operated by the national High Performance Computing (HPC) center SURFsara. All data sets and configurations ran in parallel by allocating each data set exclusively to a non-uniform memory access (NUMA) node.

5.1 Model Configuration

For the MGARCH-t model we use the package `bmgarch` (Rast & Martin, 2021) with a Student-t distribution with constant mean setting. This package is written in STAN, a Bayesian statistical inference software in C++. The priors for the MGARCH parameters are set to be uninformative and follow a uniform distribution. For the MGARCH-t model, we run every data set for 1000 iterations for 3 Markov Chains. We have realized the MGARCH-DPM model by using the `bmgarch` structure to create the custom infinite normal mixture distribution. To fit the Dirichlet mixture of the infinite normal mixture distribution we use the package `dirichletprocess` (Ross & Markwick, 2022) to create the MGARCH-DPM model as a custom Dirichlet mixture type. As the MGARCH structure is the same for both models, the MGARCH-DPM shares the same uninformative prior for the GARCH parameters. We follow MS (2021) for the prior parameters of the base measure G_0 and set $B_0 = (\nu_0 - 4)I$ such that $E(B) = I$, which centers the expectation of the conditional covariance of r_t at H_t. Moreover we set $\nu_0 = 8$, $\mu_0 = \mathbf{0}$ and $D = 0.1I$, where I denotes the 3×3 identity matrix. As initial parameters for H for the posterior estimation of Θ in Equations 50-52 we run the MGARCH-DPM for 500 warm-up iterations with $B_t = I$ and $\mu_t = \mathbf{0}$ for all $t \in \{1, \ldots, T\}$. We set $m = 3$ for the categorical new cluster draw in Equation 48.

To tune the hyperparameters for the MGARCH-DPM MCMC algorithm we perform preliminary runs for one bank (INGA NA) to evaluate the trade-off between running time, computing cost, and result improvement. The MCMC hyperparameter configuration consists of the number of Gibbs sampling iterations, the number of Metropolis-Hastings steps for the posterior update, the number of Markov Chains and the parameters for the prior distribution of α. We only explore configurations that would run in less than 6,144 System Billing Units (SBU)[5]. From our preliminary analysis of exploring 96 different configurations, we select a Metropolis-Hastings step size of 250, a gamma (2,4) prior for α, and 2 Markov Chains. Furthermore, we run our model 5 times in parallel for every portfolio for 500 iterations and chose the best in-sample performing model for our final results. To speed up convergence we update α every 5^{th} iteration and update the conditional GARCH parameters every 50^{th} or 100^{th} iteration.

[4] https://www.surf.nl/en/dutch-national-supercomputer-snellius

[5] 48 hours x 128 cores = 6,144 SBU on a thin compute node with 240 GiB of memory

5.2 Model Performance

We test the MGARCH-DPM model against the benchmark MGARCH-t model by evaluating the in-sample log-likelihood and the out-of-sample predictive log-likelihood for 3 periods consisting of 60 observations. The COVID-19 pandemic[6] and the war on Ukraine proxy as climate transition stress events and the first 60 trading days of 2019 are chosen as a control period.

Period	**Duration**	**Proxy**
Period 1	1st of January 2019 - 26st of March 2019	Control Period
Period 2	24th of January 2020 - 21st of April 2020	Climate Transition Stress Event
Period 3	24th of February 2022 - 25th of May 2022	Climate Transition Stress Event

Table 4: Periods to derive out-of-sample predictive log-likelihood.

The in-sample performance is calculated for the entire sample which lasts from the 1st of January 2010 to the 1st of August 2022. The log-likelihood for the MGARCH-t and the MGARCH-DPM model is calculated according to Equation 74 and 75, respectively. The probability distribution details for the respective kernels are found in the Appendix.

$$\ell_{MGARCH-t} = \sum_{t=1}^{T} \log\left[\mathrm{t}(r_t \mid \mu, H_t, \nu)\right] \tag{74}$$

$$\ell_{MGARCH-DPM} = \sum_{t=1}^{T} \log\left[N(r_t \mid \mu_{s_t}, (H_t^{1/2}) B_{s_t} (H_t^{1/2})')\right] \tag{75}$$

The one-step-ahead predictive likelihood is calculated for the models according to Equation 76 and 77. As the GARCH process as specified in Section 3.2 is deterministic, we can recursively compute the next conditional volatility using the conditional volatility and the observations from the previous time period. All parameter estimates for both models are displayed in Appendix K.

$$p(r_t \mid r_{1:t-1}, \text{MGARCH-t}) = \mathrm{t}(r_t \mid \mu, H_t, \nu) \tag{76}$$

For the MGARCH-DPM model, we additionally predict the mixing parameters for every observation according to Equation 78. By drawing a cluster based on probabilities proportional to the likelihood of the observation belonging to that cluster and the number of observations in a particular cluster (n_j). Additionally, in order to respect the non-parametric nature of the model, it is also possible to discover a new cluster according to Equation 79. To arrive at the predictive log-likelihood we take the summation of the one-step-ahead log-likelihoods similar to Equation 74 and 75.

[6] On the 24th of January 2020 the first COVID-19 case was confirmed in Europe.

$$p(r_t \mid r_{1:t-1}, \text{MGARCH-DPM}) = N(r_t \mid \mu_{s_t}, (H_t^{1/2}) B_{s_t} (H_t^{1/2})') \tag{77}$$

$$p(j) \propto n_j N(r_t \mid \mu_j, (H_t^{1/2}) B_j (H_t^{1/2})') \tag{78}$$

$$p(j = \text{new}) \propto \alpha \int N(r_t \mid \mu_j, (H_t^{1/2}) B_j (H_t^{1/2})') \mathrm{d}G_0 \tag{79}$$

Table 5 summarizes our results for the log-likelihoods and predictive log-likelihoods for all 7 banks applying 3 different Climate Factors across 3 periods. We compare the results for the benchmark model and our MGARCH-DPM model where a higher log-likelihood indicates a better performance. We denote the MGARCH-t model with 'M1' and our MGARCH-DPM with 'M2'. From Table 5 we find strong evidence that the MGARCH-DPM model performs better out-of-sample and in-sample as all the log-likelihoods are higher for the MGARCH-DPM model with the sole exception for period 1 for Bank of Ireland Group applying SXEPEX-SXXP as a Climate Factor.

		Log Predictive Likelihood						Log Likelihood	
		Period 1		*Period 2*		*Period 3*		*Full Sample*	
Bank Ticker		M1	M2	M1	M2	M1	M2	M1	M2
	CF_1	-317	-306*	-385	-269*	-314	-262*	-15581	-10315*
SAN SM	CF_2	-336	-225*	-371	-228*	-283	-250*	-15485	-11190*
	CF_3	-353	-219*	-288	-222*	-389	-179*	-15426	-10697*
	CF_1	-335	-304*	-306	-289*	-363	-278*	-17410	-11975*
BIRG LON	CF_2	-292*	-304	-369	-280*	-303	-286*	-17335	-13047*
	CF_3	-349	-283*	-321	-260*	-359	-323*	-17418	-14160*
	CF_1	-364	-255*	-340	-253*	-319	-268*	-15324	-10563*
BNP FP	CF_2	-296	-286*	-297	-289*	-373	-269*	-15284	-11189*
	CF_3	-305	-242*	-304	-277*	-296	-261*	-15324	-11323*
	CF_1	-279	-230*	-337	-304*	-336	-314*	-16254	-11222*
DBK GR	CF_2	-378	-223*	-319	-248*	-313	-297*	-16111	-11935*
	CF_3	-308	-197*	-287	-242*	-352	-278*	-16110	-11522*
	CF_1	-356	-262*	-321	-292*	-317	-295*	-16113	-10916*
EBS AV	CF_2	-332	-246*	-374	-233*	-300	-242*	-16098	-11715*
	CF_3	-338	-299*	-348	-232*	-339	-239*	-16043	-12289*
	CF_1	-310	-233*	-335	-221*	-350	- 249*	-15399	-9758*
INGA NA	CF_2	-307	-220*	-379	-275*	-326	-229*	-15375	-10625*
	CF_3	-264	-260*	-353	-205*	-306	-173*	-15399	-11150*
	CF_1	-312	-271*	-385	-280*	-314	-239*	-15971	-10991*
ISP IM	CF_2	-339	-261*	-340	-255*	-359	-218*	-15876	-12281*
	CF_3	-338	-236*	-396	-258*	-300	-222*	-15957	-11532*

Table 5: This table reports the predictive log-likelihood for 3 periods: Period 1 lasts from the 1st of January 2019 to the 26st of March 2019, Period 2 lasts from 24th of January 2020 to the 21st of April 2020 and Period 3 lasts from the 24th of February 2022 to the 25th of May 2022 (all 60 observations). The log-likelihood is reported on the entire estimation period, which corresponds to the 1st of January 2010 to the 1st of August 2022. Model 1 (M1) refers to the MGARCH-t model and model 2 (M2) refers to MGARCH-DPM model. The models are fitted on daily return data of the respective bank, the market factor SXXP and one of the 3 Climate Factors: CF_1 OIL - SXXP, CF_2 SXEPEX - SXXP, CF_3 XEPS - SXXP. The * indicates which method performed better.

5.3 Climate Beta Results

In this section, we discuss the Climate Beta results generated by the MGARCH-t model and our MGARCH-DPM model. Figure 1 depicts the Climate Beta results for the period from 1st of January 2018 to the 1st of August 2022 for both methods averaged over all Climate Factors for 3 climate stress severities (Appendix Figure 4 depicts the comparison for the entire period from the 1st of January 2010 to the 1st of August 2022). Appendix Figure 6 depicts the Climate Beta results for the MGARCH-t model for every Climate Factor. The same is found in Appendix Figure 7 for the MGARCH-DPM model.

We expand the work of JEB and investigate the climate stress resilience of Eurozone banks for three climate stress scenarios: a 30%, 50% and 70% decline in the stranded-asset portfolio. Recalling Equation 9 from the MGARCH-DPM model, we allow the Climate Beta to depend on the climate stress severity. As the MGARCH-t estimated Climate Beta is constant with respect to the climate stress severity, we do not perform separate computations for each climate stress event. From Figure 1 we do not observe a non-linear response of the Climate Beta for the MGARCH-DPM model for both climate stress proxy periods conditional on the 3 climate stress scenarios. Furthermore, the Climate Beta does not display a non-linear effect during the non-stressed control period. The same conclusion applies to the entire period as depicted in Appendix Figure 4.

A positive Climate Beta indicates that a bank is negatively affected by the downturn of the stranded asset portfolio and, vice versa, a negative Climate Beta signals a positive response to the devaluation of the stranded asset portfolio. For the majority of the estimation period MGARCH-t Climate Beta fluctuates between a range of -1 to 1, which is roughly in line with what JEB find for banks investigated in their paper. In contrast, the nonparametric dynamic conditional Climate Beta oscillates between an expanded range and estimates a Climate Beta in the climate stress event as high as 2.5. This would imply that a 1% fall in the stranded asset portfolio induces a 2.5% fall in the bank return.

When comparing the averaged Climate Beta estimates, we identify two groups of banks with regard to their Climate Beta trend. For one group, the Climate Beta across both models seems to follow an identical pattern (with the exception of the Climate Beta during March 2020). Banco Santander, S.A., BNP Paribas S.A., and Deutsche Bank AG fall into this group and also correspond to the three largest banks of this analysis. For the other banks, the MGARCH-DPM estimated Climate Beta is consistently lower than the Climate Beta estimated by the MGARCH-t model. The divergence of the MGARCH-t Climate Beta and MGARCH-DPM Climate Beta with respect to the sign of the Climate Beta is striking, as this shifts the conclusion of the sensitivity to the stranded-asset portfolio. This signals that by relaxing all distributional assumptions, such as symmetry and thickness of tails, the MGARCH-DPM model is able to model a richer dependence compared to the restricted MGARCH-t model.

Figure 1: A Climate Beta cross-method comparison for the period from the 1st of January 2018 to 1 of August 2022. M1 refers to MGARCH-t. M2 refers to MGARCH-DPM: M2 0.3 refers to the Climate Beta conditional on a contemporaneous Climate Factor return of -0.3 ($\theta = 0.3$). Idem dito for M2 0.5 and M2 0.7. The Climate Beta is computed by taking the average Climate Beta over all three Climate Factors.

Before March 2020, the Climate Beta appears relatively stable for all banks and does not seem to exhibit an anticipatory positive trend before the aforementioned period. Recalling that the Covid-19 crisis is chosen as a climate stress event due to the similarities to the climate transition stress scenarios. We noted earlier that the banks could be divided into two groups with the exception of the Climate Beta in March 2020: during this period the Climate Beta is positive for all banks. For this period it is apparent from Figure 1 that the MGARCH-DPM model estimates a more volatile Climate Beta. However, the positive peak is temporary and does not persist. While the control period still displays some idiosyncrasies in the Climate Beta, the identical response across all banks during the initial Covid-19 period supports the systemic nature of climate change risk. A peak of similar intensity is not observed during February 2022. Moreover, we observe a moderate upward trend in the Climate Beta across both models starting from February 2022, again with the exception for Erste Group Bank AG. For the latter bank, the Climate Beta stabilizes and only for February displays an aberration and exhibits a negative peak for both models. Solely for Deutsche Bank AG, the MGARCH-DPM model estimates a moderate positive peak during February 2022.

With regards to the different Climate Factors, we only observe discrepancies in Climate Betas for Bank of Ireland Group plc and ING Groep N.V. for the MGARCH-DPM model. Both banks react similarly, where for both banks saw Climate Factor 3 as having the highest Climate Beta, followed by Climate Factor 2 and lastly Climate Factor 1. This discrepancy is only observed for the MGARCH-DPM model and is depicted in Appendix Figure 7. Although for the majority of the banks one Climate Factor would suffice, for the two banks named earlier the resulting CRISK differs significantly among the Climate Factor. Therefore, we suggest that more than one Climate Factor is necessary to compute the Climate Beta to prevent biased results.

5.4 CRISK Results

In this section, we present the CRISK results applying a Climate Beta generated by the MGARCH-t and the MGARCH-DPM model. As we did not find evidence of non-linear contemporaneous Climate Beta dynamics, we continue by computing CRISK for both methods for a climate stress severity of $\theta = 0.5$. Figure 2 depicts the CRISK for all banks for both the MGARCH-t and the MGARCH-DPM model across the entire estimation period averaged over all Climate Factors. Appendix Figure 10 and 11 exhibit the CRISK for the entire estimation period for each Climate Factor for the MGARCH-t and the MGARCH-DPM model, respectively. Figure 3 depicts the results for the period from 1st of January 2018 to the 1st of August 2022 for both methods averaged over all Climate Factors (Appendix Figure 5 depicts the comparison for the entire period from the 1st of January 2010 to the 1st of August 2022). Appendix Figure 8 depicts the CRISK results for the MGARCH-t model for every Climate Factor. Likewise, the CRISK results for every Climate Factor are exhibited for the MGARCH-DPM model in Appendix Figure 9.

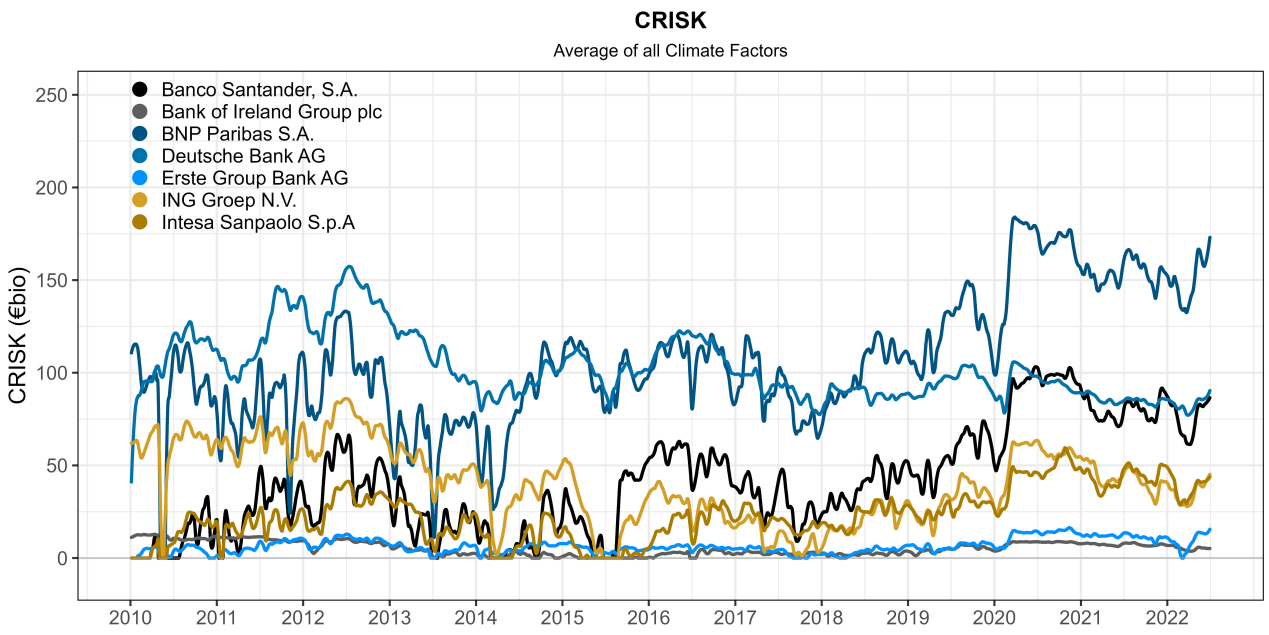

(a) CRISK MGARCH-t computed with $\theta = 0.5$

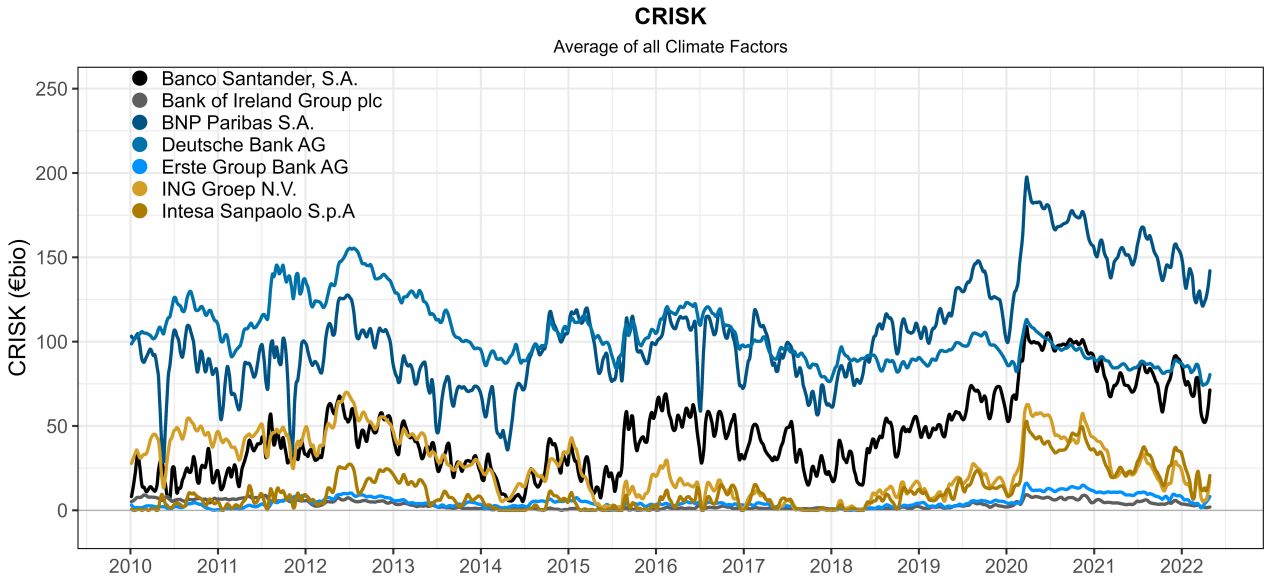

(b) CRISK MGARCH-DPM computed with $\theta = 0.5$

Figure 2: CRISK for Eurozone Banks conditioned on a 50% decline in the Climate Factor.

From Figure 2 we conclude that while the Climate Beta varies among the MGARCH-t and MGARCH-DPM model, the averaged CRISK results follow a similar trend with discrepancies revealed only upon close inspection. Zooming in on the period 2018-2022 in Figure 3, it is clear how the banks form pairs based on their CRISK pattern. Banco Santander, S.A. and BNP

Parisbas S.A. follow an identical pattern, the same applies to Erste Group Bank AG and Intesa Sanpaolo S.p.A., and lastly Bank of Ireland Group plc and ING Groep N.V. Hence the pairs seem to be based on proximity to each other. Only Deutsche Bank AG tends to deviate from the other banks in this respect. Remarkably, the pairs do not only match in their CRISK pattern, but also in their response to the different Climate Factors as seen in Figure 9. The most notable example being ING Groep N.V. and Bank of Ireland Group plc.

Comparing both models individually in Figure 3, we observe a steep jump in CRISK for most banks during the initial period of Covid-19 in March 2020 as hypothesized. From the intensity of the jump, we can sense the sensitivity of CRISK to the Climate Beta. It is compelling to observe that a jump in the Climate Beta, as noted in the previous section, does not translate to a jump of similar intensity in CRISK. This suggests that the forces of debt and equity dominate CRISK over the effect exerted by the Climate Beta during this period. An explanation for this could be that banks operate on a high Debt-to-Equity ratio compared to other types of institutions. It may also be bolstered by the fact that the value of debt is assumed not to change in a climate stress scenario as per the definition of CRISK and is therefore not weighted by the Climate Beta.

Furthermore, the dominant effect of debt could insinuate that even in a non-stressed scenario most of the banks would experience a positive CRISK regardless of the applied climate stress severity. Broadening our view over the entire estimation period in Figure 2 and Figure 9 furthers our suspects of the presiding role of the balance sheet input in CRISK. Most banks experience a positive CRISK for the entire estimation period, whereas not all years are identified as climate stress proxy periods. As capital shortfall during these periods would not be catalyzed by a climate stress event, it raises the question of whether the definition of CRISK fits its purpose of measuring the climate stress induced capital shortfall. We suggest that there should be more focus on the difference in CRISK between stressed and non-stressed capital shortfall to further isolate the climate transition stress effect.

Continuing post-March 2020, we note a downward trend for all banks until February 2022. We observe that by early 2022 some of the banks have returned to their original CRISK level in the case of the MGARCH-DPM estimated Climate Beta. The MGARCH-t estimate Climate Beta seems to have offset more of a level shift in CRISK. February 2022 marks again an upward trend for all banks except for Bank of Ireland plc. Erste Bank Group AG reacts strongest to the period and exhibits a steep jump in CRISK. However, this upward trend does not seem to be caused in response to a climate transition stress event as the Climate Beta revolves around 0 for all banks. The ambivalence of the Climate Beta during this period hints that the rise in CRISK is due to a fall in market capitalization. Although we do not want to rule out this period as a climate transition proxy, our analysis does not find supporting evidence that the period in question is distressed in CRISK due to transition risk given the studied Climate Factors.

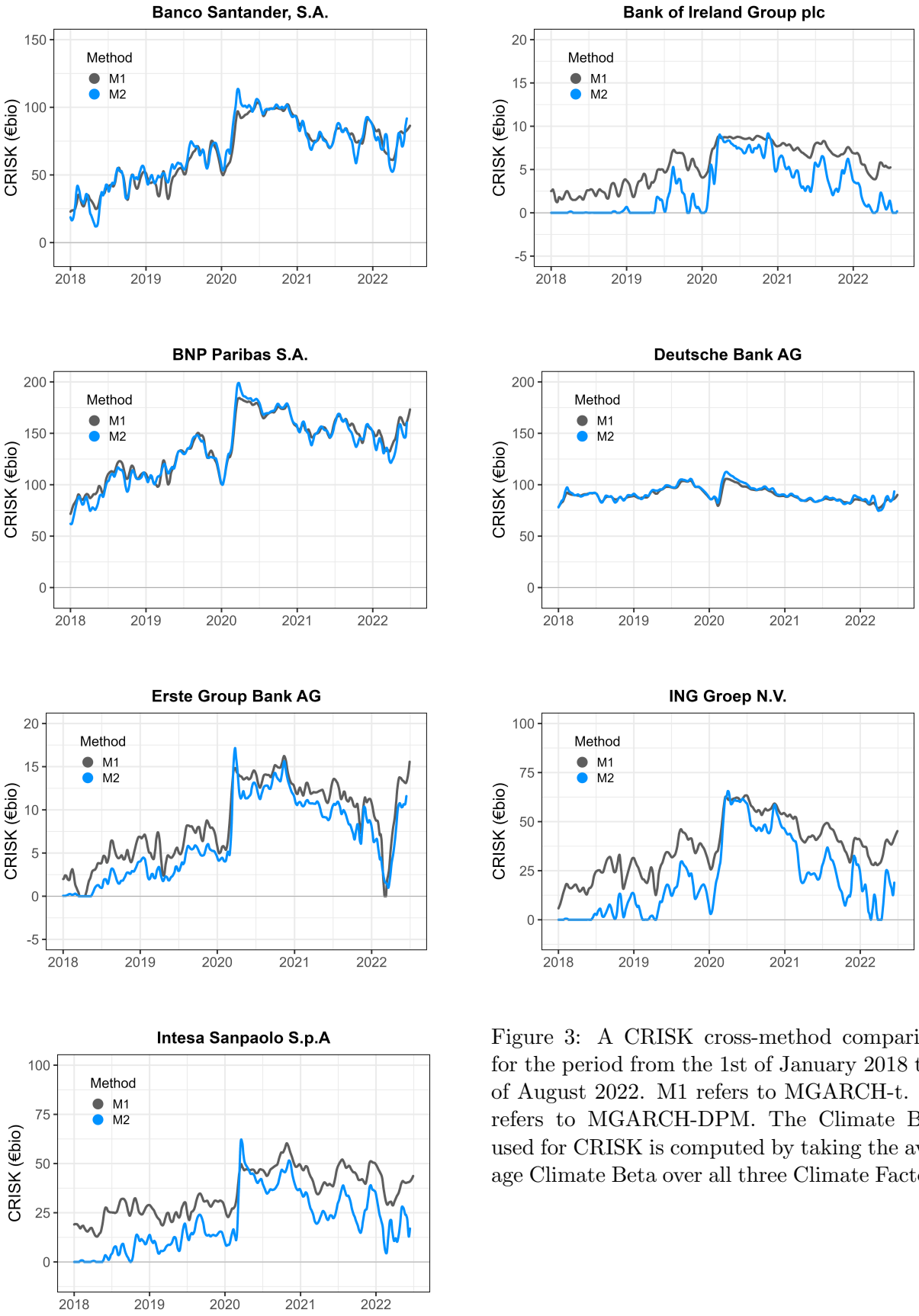

Figure 3: A CRISK cross-method comparison for the period from the 1st of January 2018 to 1 of August 2022. M1 refers to MGARCH-t. M2 refers to MGARCH-DPM. The Climate Beta used for CRISK is computed by taking the average Climate Beta over all three Climate Factors.

6 Conclusion

Our paper expands the work of Jung, Engle and Berner on CRISK, a risk metric that attempts to gauge the climate transition resilience of a financial institution. CRISK measures the capital shortfall conditional on a hypothetical climate transition stress scenario by merging the book value of debt, the market value of equity and a Climate Beta. The latter variable corresponds to the sensitivity of a bank to a climate transition proxy, which in our case is a stranded asset portfolio or also named a Climate Factor. This is chosen according to the assumption that the devaluation in stranded assets, such as oil and coal, mimics a climate transition stress scenario. The effect exerted by the Climate Beta could decrease the bank's required capital and induce a capital shortfall.

The novelty of our research is twofold: we extended the work on CRISK both in the scope of our analysis as well as in the applied methodology. First, we performed a Eurozone-focused analysis by examining the CRISK of 7 of the largest European banks. Continuing, we advanced the robustness of CRISK by exploring 3 stranded asset portfolios where the stranded assets investigated are OIL FP, SXEPEX GR and XEPS GY. Moreover, we explored 3 climate stress severities: a 30%, 50% and 70% devaluation in the Climate Factor over a course of 6 months. Second, this study proposed a novel approach to the estimation of the Climate Beta in CRISK. We proposed a non-parametric dynamic conditional Climate Beta which depends non-linearly on the climate stress severity. To derive the non-parametric Climate Beta, we relaxed the distributional assumptions on the joint returns and modeled the density according to an infinite normal mixture model. As a result of our methodology, we introduced a new definition of CRISK whereby the Climate Beta is conditional on the climate stress event.

We modeled our infinite normal mixture model using a Dirichlet prior following Maheu & Shamsi (2021), where the mixing occurs over the mean and the conditional covariance. To realize the Dirichlet process mixture, we used a 'Chinese Restaurant Process' with Gibbs sampling. Moreover, we used a semi-conjugate prior for the base distribution of the Dirichlet process and applied a Metropolis-Hastings step within the Gibbs sampling to re-sample the mixing parameters. We compared our non-parametric infinite normal mixture model to our parametric benchmark model, which concerns a Student-t distribution with a constant mean and conditional scale matrix. We used DCC parametrization for the MGARCH process in both models (Engle, 2002). The Climate Beta was extracted according to the DCB methodology (Engle, 2015).

We performed an estimation for the period from the 1st of January 2010 to the 1st of August 2022. To test the model performance out-of-sample, we formed three prediction periods: 1) a control period corresponding to the first 60 days of 2019; 2) the first 60 days of the Covid-19 crisis resembling a climate transition stress event driven by a contraction in demand due to a drop in consumer confidence; and 3) the first 60 days of the Ukraine war resembling a climate transition

stress scenario due to an increased price of carbon-intensive assets. We conclude that the MGARCH-DPM performs better both in- and out-of-sample based on the log-likelihood and predictive log-likelihood.

One key insight from our research is that the non-parametric dynamic conditional Climate Beta is more sensitive to a climate transition stress event. We observed for all Eurozone banks that the MGARCH-DPM estimated Climate Beta is more volatile and has a stronger response to the Covid-19 crisis. As the MGARCH-DPM model provides a better in- and out-of-sample fit to the data compared to the MGARCH-t model, we conclude that the parametric Climate Beta underestimates the sensitivity of a bank to a climate transition stress event. Furthermore, the better performance of the MGARCH-DPM model suggests that the symmetric distributional assumption of the benchmark model is invalid and underestimates the tail of the distribution. As tail risk is critical in the study of systemic crisis events, our results underline the importance of distribution precaution towards estimating climate change risk.

More so, we applied a non-parametric dynamic conditional Climate Beta to examine a possible non-linear response of the Climate Beta conditional on the different climate stress scenarios. We did not detect that the MGARCH-DPM Climate Beta responds non-linearly to the climate stress severities in question for the considered time period. This could be further investigated as Maheu & Shamsi (2021) do find a non-linear response to a market beta for banks in the United States. Furthermore, inspecting the early 2010s, it is clear that the Climate Beta picks up on market sentiment during the late financial crisis. This does challenge the stranded-asset portfolio as a fit to measure only climate transition risk. We suggest more quantitative and qualitative research could be done to further differentiate the climate change effect from a market effect.

While the empirical results strongly encourage our non-parametric model to describe the data, at the same time we emphasize the computational intensity of the posterior inference. The depth of our analysis would not have been feasible without access to the supercomputer Snellius. The strenuous computation of the MGARCH-DPM model could preclude banks and supervisory institutions to update the non-parametric Climate Beta on a daily basis. We thus suggest that the non-parametric Climate Beta and CRISK be updated weekly or monthly. This poses a limitation to the practicality of the MGARCH-DPM model and we suggest further research to look into improving the efficiency of the posterior inference of the infinite normal mixture model. For example, future research could look into exchanging the semi-conjugate prior with a conjugate prior for the base measure of the Dirichlet process. This would eliminate the need for a Metropolis step and could therefore speed up convergence.

On a final note, we conclude that all Eurozone banks are subject to CRISK throughout the entire estimation period. The Covid-19 crisis marked a steep jump in CRISK across all banks and we also observed an upward trend from the start of the war on Ukraine in February 2022. However, this effect was not merely as intense as in March 2020. Therefore, we conclude that a climate

transition stress event of the nature of Covid-19 has a stronger effect on capital shortfall compared to that of the war on Ukraine. During the first climate transition proxy period, we noted positive Climate Betas as hypothesized. On the other hand, we note that during the second transition proxy period the Climate Betas are tending towards zero. This challenges February 2022 as a climate transition stress event. Furthermore, this also challenges the definition of CRISK as the capital shortfall conditional on a climate stress event. This brings us to another key insight of our research as we observed that CRISK is also positive during non-stressed periods. Therefore, we conclude that CRISK is mostly dependent on the value of debt and equity, and that the Climate Beta does not exert a significant effect. This is supported by the observation that most European banks are already in capital distress without a climate transition event. We thus suggest further research on isolating climate stress-induced capital shortfall.

References

Acharya, V. V., Pedersen, L. H., Philippon, T., & Richardson, M. P. (2010). Measuring systemic risk. *SSRN Electronic Journal*.

Alogoskoufis, S., Dunz, N., Emambakhsh, T., Hennig, T., Kaijser, M., Kouratzoglou, C., ... Salleo, C. (2021). Ecb economy-wide climate stress test. *ECB Occasional Paper Series*(291).

Battiston, S., Mandel, A., Monasterolo, I., Schütze, F., & Visentin, G. (2017). A climate stress-test of the financial system. *Nature Climate Change*(7), 283–288.

Bollerslev, T. (1986). Generalized autoregressive conditional heteroskedasticity. *Journal of Econometrics*, *31*(3), 307-327.

Bollerslev, T., Engle, R. F., & Wooldridge, J. M. (1988). A capital asset pricing model with time-varying covariance. *Journal of Political Economy*, *96*(1), 116-131.

Brownlees, C., & Engle, R. F. (2018). Srisk: A conditional capital shortfall measure of systemic risk. *The Review of Financial Studies*, *30*(1), 48-79.

ECB/ESRB. (2021). *Climate-related risk and financial stability.* European System of Financial Supervision.

Engle, R. F. (1982). Autoregressive conditional heteroskedasticity with estimates of the variance of u.k. inflation. *Econometrica*, *50*(4), 987-1008.

Engle, R. F. (2002). Dynamic conditional correlation: A simple class of multivariate generalized autoregressive conditional heteroskedasticity models. *Journal of Business & Economic Statistics*, *20*(3), 339-350.

Engle, R. F. (2015). Dynamic conditional beta. *SSRN Electronic Journal*.

Engle, R. F. (2018). Systemic risk 10 years later. *Annual Review of Financial Economics*, *10*(1), 125-152.

Engle, R. F., & Kroner, K. F. (1995). Multivariate simultaneous generalized arch. *Econometric Theory*, *11*(1), 122-150.

Escobar, M. D., & West, M. (1995). Bayesian density estimation and inference using mixtures. *Journal of the American Statistical Association*, *90*(430), 577-588.

Ferguson, T. S. (1973). A bayesian analysis of some nonparametric problems. *The Annals of Statistics*, *1*(2), 209-230.

Garnier, J., Gaudemet, J.-B., & Gruz, A. (2022). The climate extended risk model (cerm). *SSRN Electronic Journal*.

Gelfand, A. E., & Smith, A. F. M. (1990). Sampling-based approaches to calculating marginal densities. *Journal of the American Statistical Association*, *85*(410), 398-409.

Geman, S., & Geman, D. (1984). Stochastic relaxation, gibbs distributions, and the bayesian restoration of images. *IEEE Transactions on Pattern Analysis and Machine Intelligence*, *PAMI-6*(6), 721-741.

Hastings, W. K. (1970). Monte carlo sampling methods using markov chains and their applications. *Biometrika Trust*, *57*(1), 97-230.

Huij, J., Laurs, D., Stork, P., & Zwinkels, R. C. (2022). Carbon beta: A market-based measure of climate risk. *SSRN Electronic Journal*.

Ishwaran, H., & James, L. F. (2001). Gibbs sampling methods for stick-breaking priors. *Journal of the American Statistical Association*, *96*(453), 161-173.

Jung, H., Engle, R., & Berner, R. (2021). Climate stress testing. *Federal Reserve Bank of New York Staff Report*, *977*.

Kenyon, C., & Berrahoui, M. (2021). Climate change valuation adjustment (ccva) using parameterized climate change impacts. *SSRN Electronic Journal*.

Li, D., Clements, A., & Drovandi, C. (2021). Efficient bayesian estimation for garch-type models via sequential monte carlo. *Econometrics and Statistics*, *19*(C), 22-46.

Maheu, J. M., & Shamsi, A. (2021). Nonparametric dynamic conditional beta. *Journal of Financial Econometrics*, *19*(4), 583-613.

Marco, M., & Jiron, A. (2020). Sriskv2 - a note. *FEDS Notes*.

Metropolis, N., Rosenbluth, A. W., Rosenbluth, M. N., Teller, A. H., & Teller, E. (1953). Equation of state calculations by fast computing machines. *The Journal of Chemical Physics*, *21*(6), 1087-1092.

Neal, R. M. (2000). Markov chain sampling methods for dirichlet process mixture models. *Journal of Computational and Graphical Statistics*, *9*(2), 249-265.

Ojea-ferreiro, J., Rebordedo, J. C., & Ugolini, A. (2022). The impact of climate transition risks on financial stability. a systemic risk approach. *JRC Working Papers in Economics and Finance*.

Papaspiliopoulos, O., & Roberts, G. O. (2008). Retrospective markov chain monte carlo methods for dirichlet process hierarchical models. *Biometrika*, *95*(1), 169–186.

Rast, P., & Martin, S. (2021). bmgarch: Bayesian multivariate garch models [Computer software manual]. Retrieved from https://CRAN.R-project.org/package=bmgarch (R package version 1.1.0)

Ross, G. J., & Markwick, D. (2022). dirichletprocess: Build dirichlet process objects for bayesian modelling [Computer software manual]. Retrieved from https://CRAN.R-project.org/package=dirichletprocess (R package version 0.4.0)

Vermeulen, R., Schets, E., Lohuis, M., Kölbl, B., Jansen, D.-J., & Heeringa, W. (2018). An energy transition risk stress test for the financial system of the netherlands. *De Nederlandsche Bank N.V. Occasional Studies*, *16*(7).

Vinciguerra, O., & Gaudemet, J.-B. (2020). How banks can save the planet. *Green RWA*(1).

Walker, S. G. (2007). Sampling the dirichlet mixture model with slices. *Communications in Statistics - Simulation and Computation*, *36*(1), 45-54.

West, M. (1992). Hyperparameter estimation in dirichlet process mixture models. *Duke University, ISDS*, *92*(A03).

A Acronyms

ARMA Auto Regressive Moving Average.

ASRF Asymptotic Single Risk Factor.

AUM Assets Under Management.

BCBS Basel Committee on Banking Supervision.

CCVA Climate Change Valuation Adjustment.

CERM Climate Extended Risk Model.

CRP Chinese Restaurant Process.

CS Capital Shortfall.

CTER Climate Transition Expected Return.

CTES Climate Transition Expected Shortfall.

CTVAR Climate Transition Value-at-Risk.

CVA Credit Valuation Adjustment.

DCB Dynamic Conditional Beta.

DCC Dynamic Conditional Correlation.

DNB De Nederlandsche Bank.

DPM Dirichlet Process Mixture.

EBA European Banking Authority.

ECB European Central Bank.

ESG Environmental, Social, and Governance.

ESRB European Systemic Risk Board.

ETF Exchange Traded Funds.

FVA Funding Valuation Adjustment.

GARCH Generalized AutoRegressive Conditional Heteroskedasticity.

HPC High Performance Computing.

IRB Internal Ratings-Based.

ITS Implementing Technical Standards.

JEB Hyeyoon Jung, Robert Engle, and Richard Berner.

LRMES Long-Run-Marginal Expected Shortfall.

MCMC Markov Chain Monte Carlo.

MGARCH Multivariate Generalized Autoregressive Conditional Heteroskedasticity.

MS John M. Maheu and Azam Shamsi.

NUMA Non-Uniform Memory Access.

PMC Pollutive-Minus-Clean.

RWA Risk-Weighted-Assets.

SBU System Billing Units.

SREP Supervisory Review and Evaluation Process.

WRDS Wharton Research Data Services.

B Distributions

Multivariate Student-t distribution

If $\mathbf{x} \sim t(\mu, \Sigma, \nu)$ then the density function of the multivariate Student-t distribution is:

$$t(\mathbf{x} \mid \nu, \mu, \Sigma) = \frac{\Gamma\left(\frac{\nu+p}{2}\right)}{\Gamma\left(\frac{\nu}{2}\right)\pi^{p/2}}|\Sigma|^{-1/2}\left[1+\frac{1}{\nu}(\mathbf{x}-\mu)^T\Sigma^{-1}(\mathbf{x}-\mu)\right]^{-(\nu+p)/2}, \nu > 0.$$

Where p denotes the dimension of x, μ denotes the $p \times 1$ location vector, Σ denotes the positive-definite $p \times p$ scale matrix, and ν denotes the degrees of freedom.

Multivariate Normal distribution

If $\mathbf{x} \sim N(\mu, \Sigma)$ then the density function of the multivariate normal distribution is:

$$N(\mathbf{x} \mid \mu, \Sigma) = \frac{1}{\sqrt{(2\pi)^p|\Sigma|}}\exp\left(-\frac{1}{2}(\mathbf{x}-\mu)^T\Sigma^{-1}(\mathbf{x}-\mu)\right).$$

Where p denotes the dimension of x, μ denotes the $p \times 1$ location vector and Σ denotes the positive semi-definite $p \times p$ covariance matrix.

Inverse Wishart distribution

If $\mathbf{X} \sim \mathcal{W}^{-1}(\Psi, \nu)$ where $\mathbf{X}$ is an $p \times p$ matrix, follows an inverse Wishart density with a positive-definite scale matrix Ψ and degree of freedom $\nu \geq p+1$, the density function equals:

$$\mathcal{W}^{-1}(\mathbf{X} \mid \Psi, \nu) = \frac{|\Psi|^{\nu/2}}{2^{\frac{p\nu}{2}}\pi^{\frac{p(p-1)}{4}}\Pi_{i=1}^{p}\Gamma\left(\frac{\nu+1-i}{2}\right)}|\mathbf{X}|^{-\frac{\nu+p+1}{2}}\exp\left[-\frac{1}{2}\operatorname{tr}\left(\Psi\mathbf{X}^{-1}\right)\right]$$

Gamma distribution

The probability density function of the Gamma distribution with shape parameter α and scale parameter β is given by:

$$\mathcal{G}(x \mid \alpha, \beta) = \frac{\beta^\alpha}{\Gamma(\alpha)}x^{\alpha-1}e^{-\beta x}, \alpha > 0, \beta > 0.$$

C Climate Beta Method Comparison

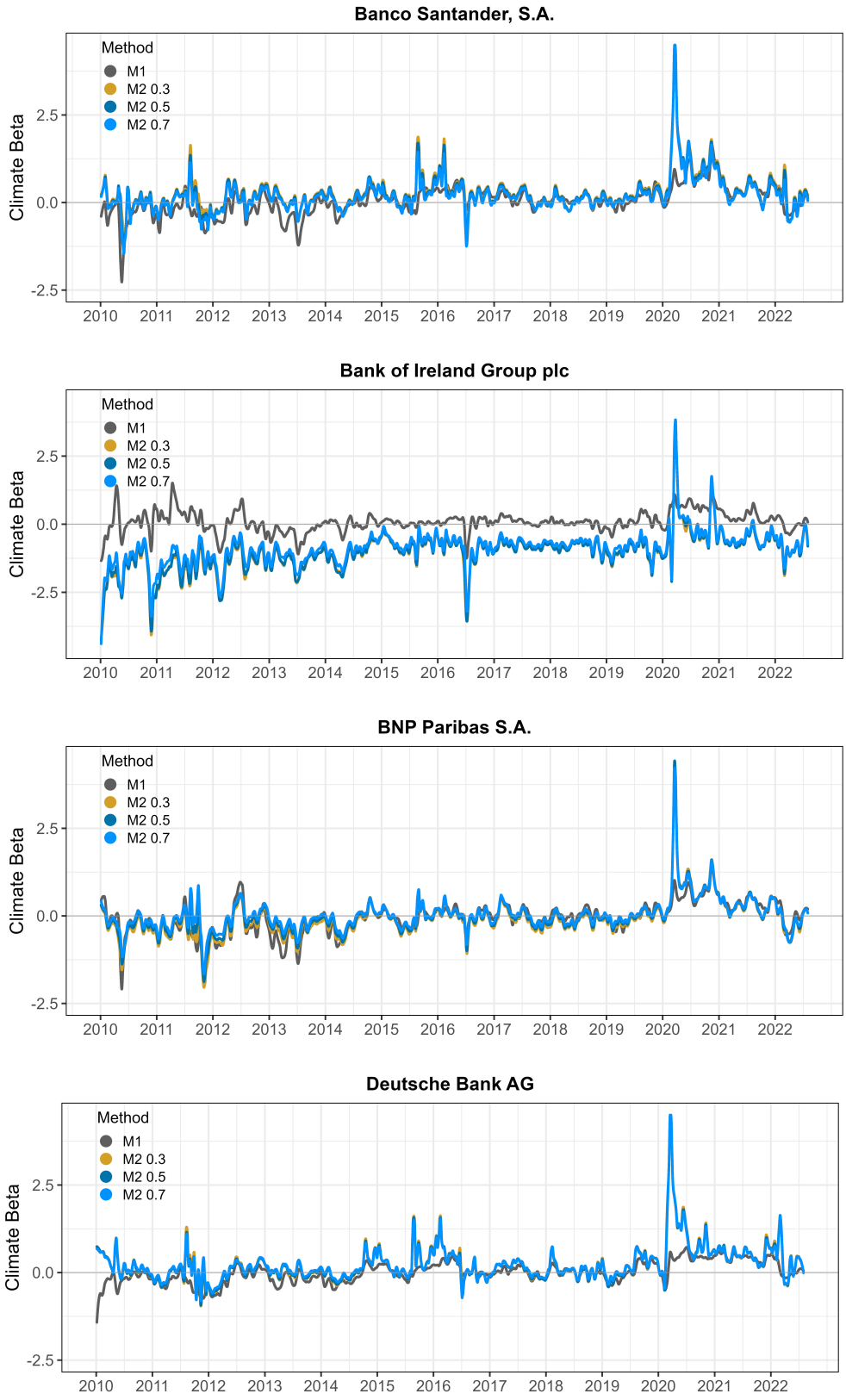

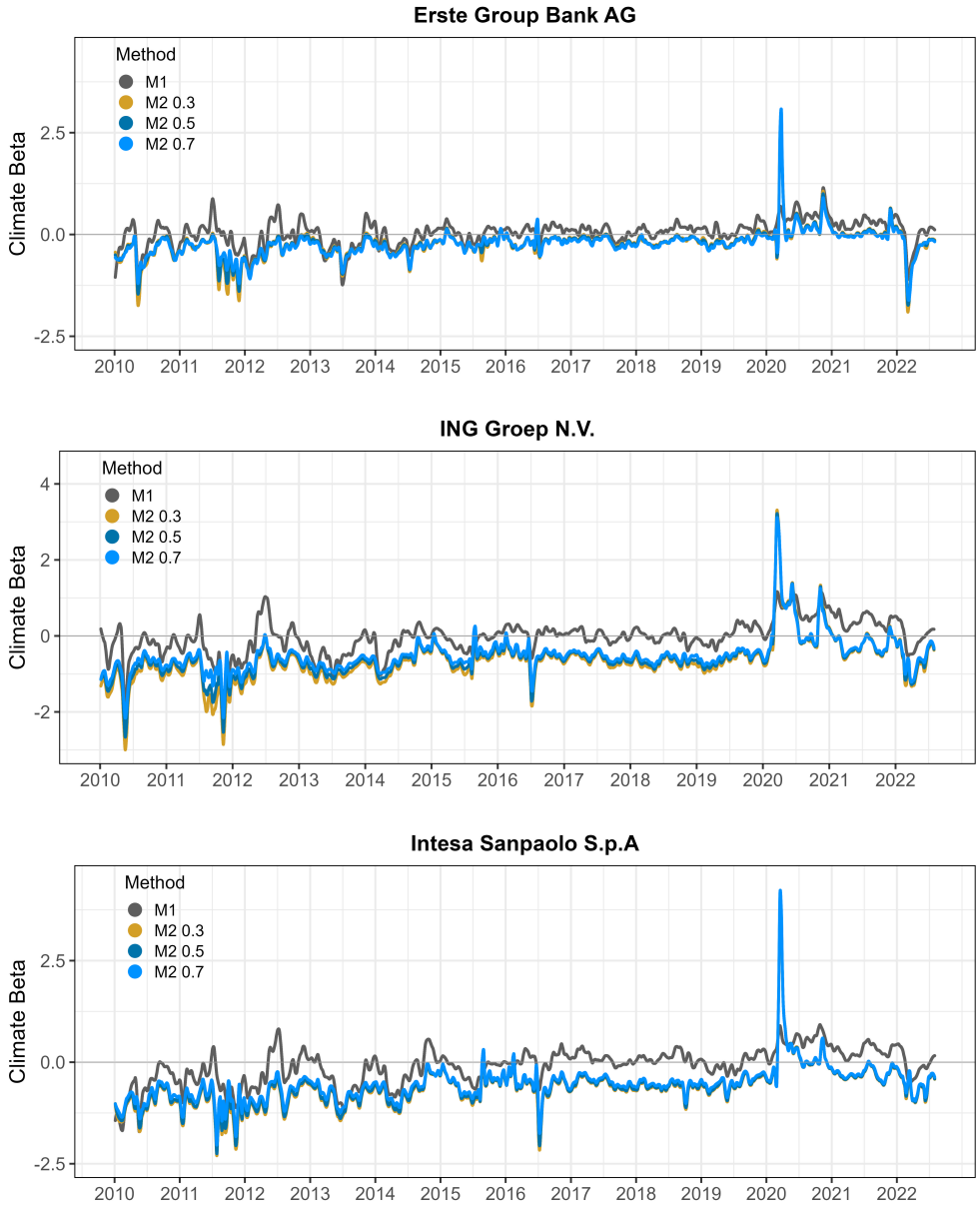

Figure 4: A Climate Beta cross-method comparison for the period from the 1st of January 2010 to 1 of August 2022. M1 refers to MGARCH-t. M2 refers to MGARCH-DPM: M2 0.3 refers to the Climate Beta conditional on a climate stress severity $\theta = 0.3$. Idem dito for M2 0.5 and M2 0.7.

D CRISK Method Comparison

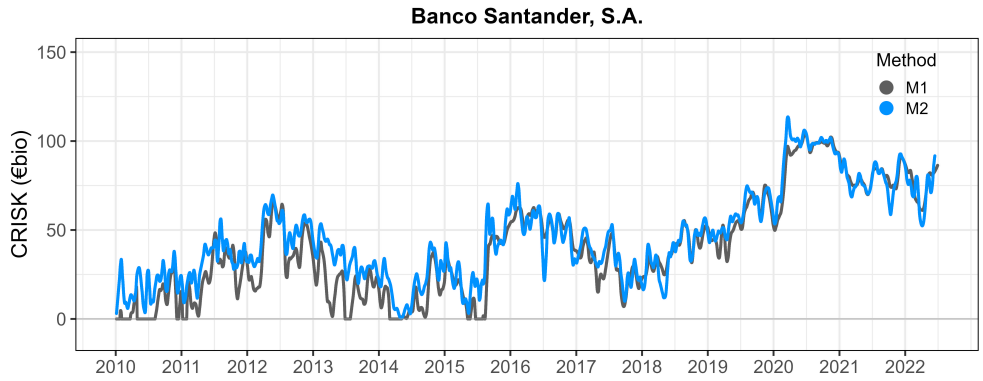

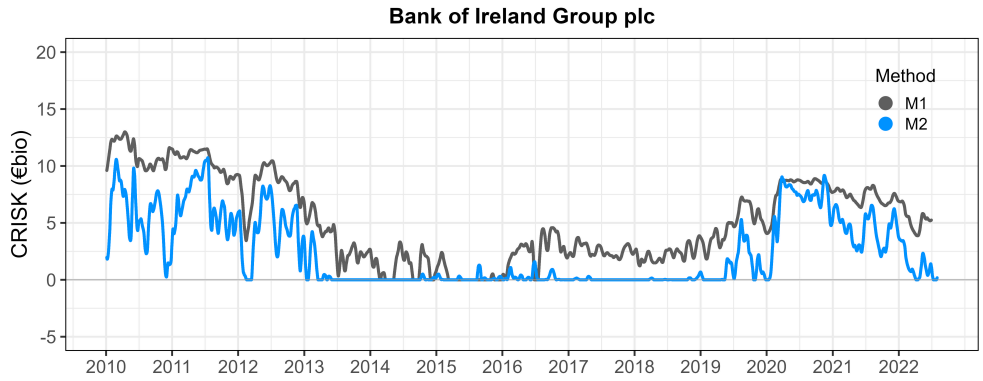

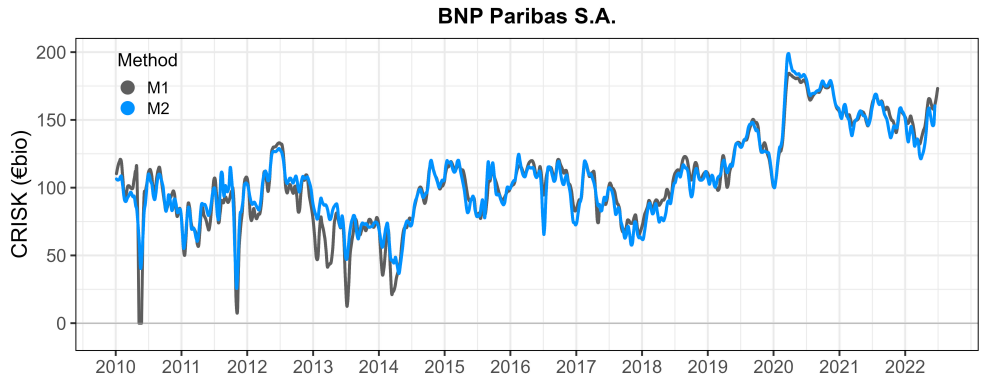

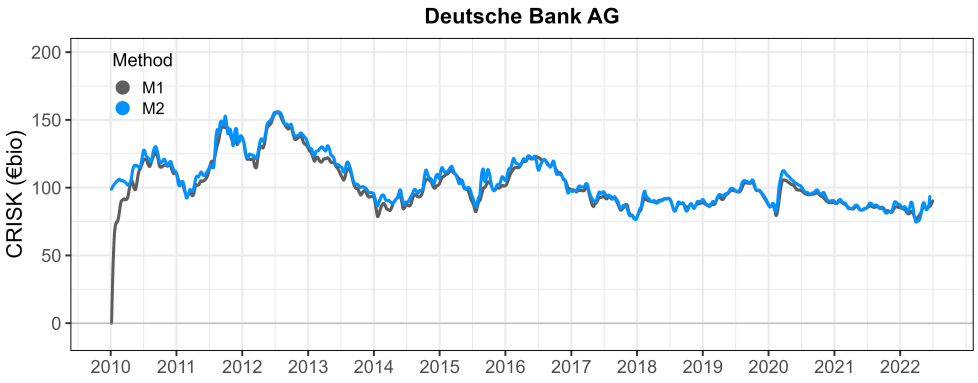

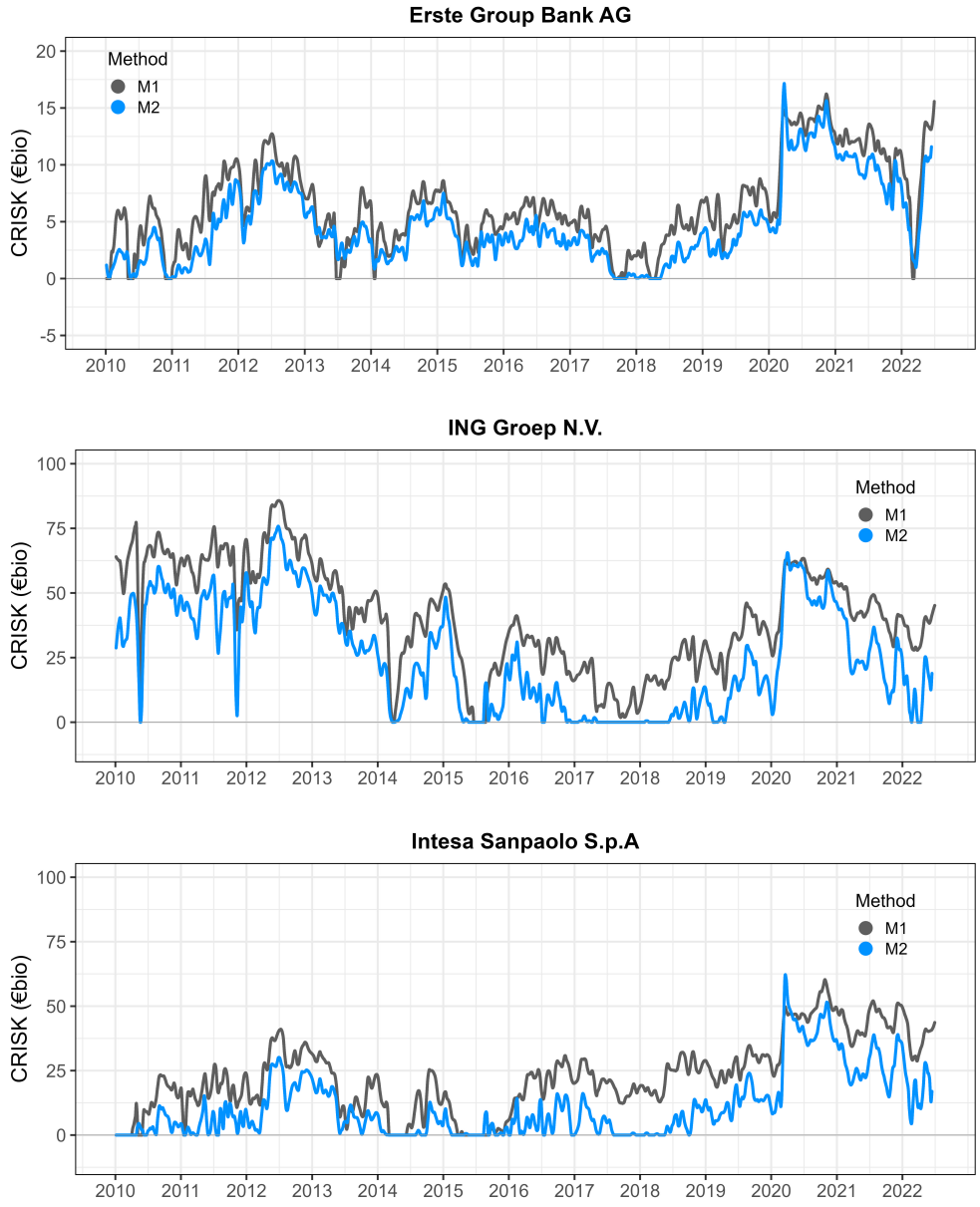

Figure 5: A CRISK cross-method comparison for the 1st of January 2010 to 1st of August 2022. M1 refers to MGARCH-t. M2 refers to MGARCH-DPM. CRISK is computed with a climate stress severity of $\theta = 0.5$

E MGARCH-t Individual Climate Beta

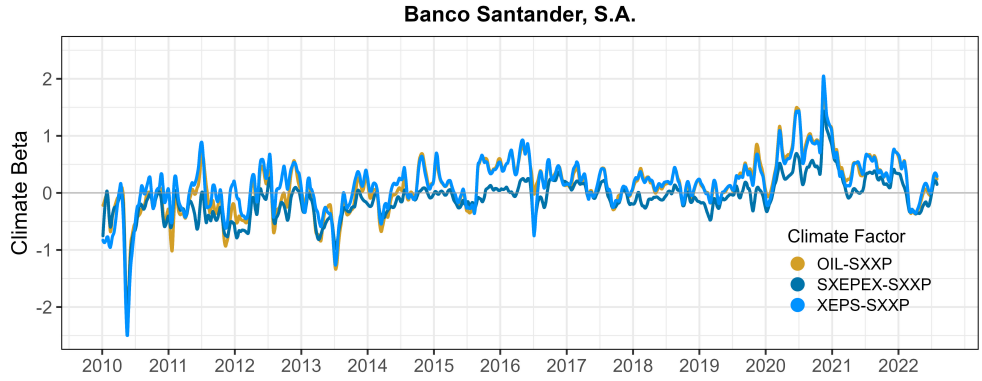

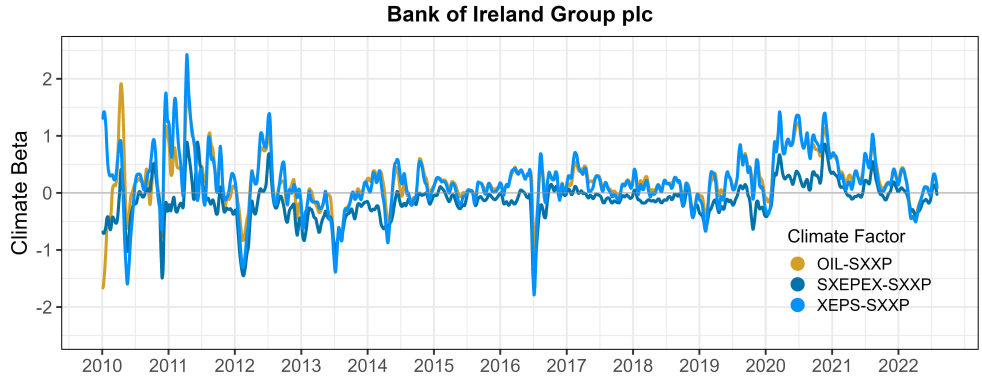

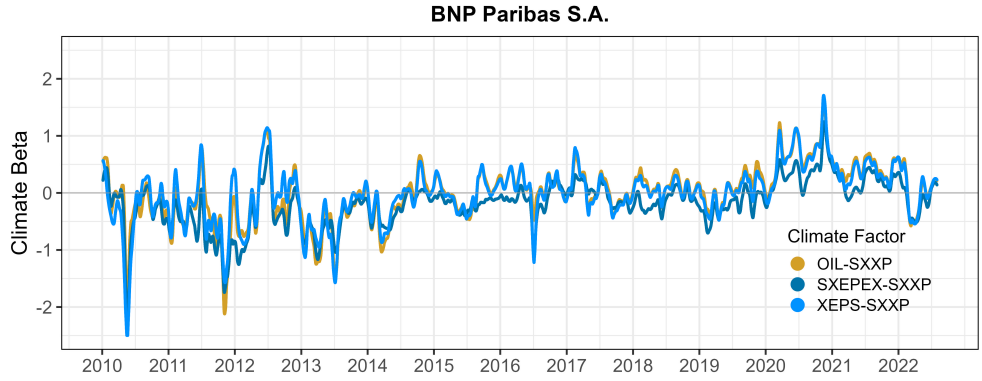

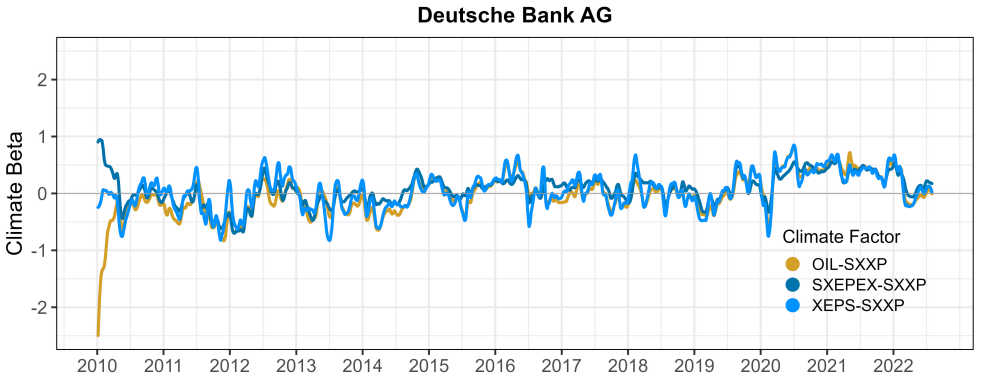

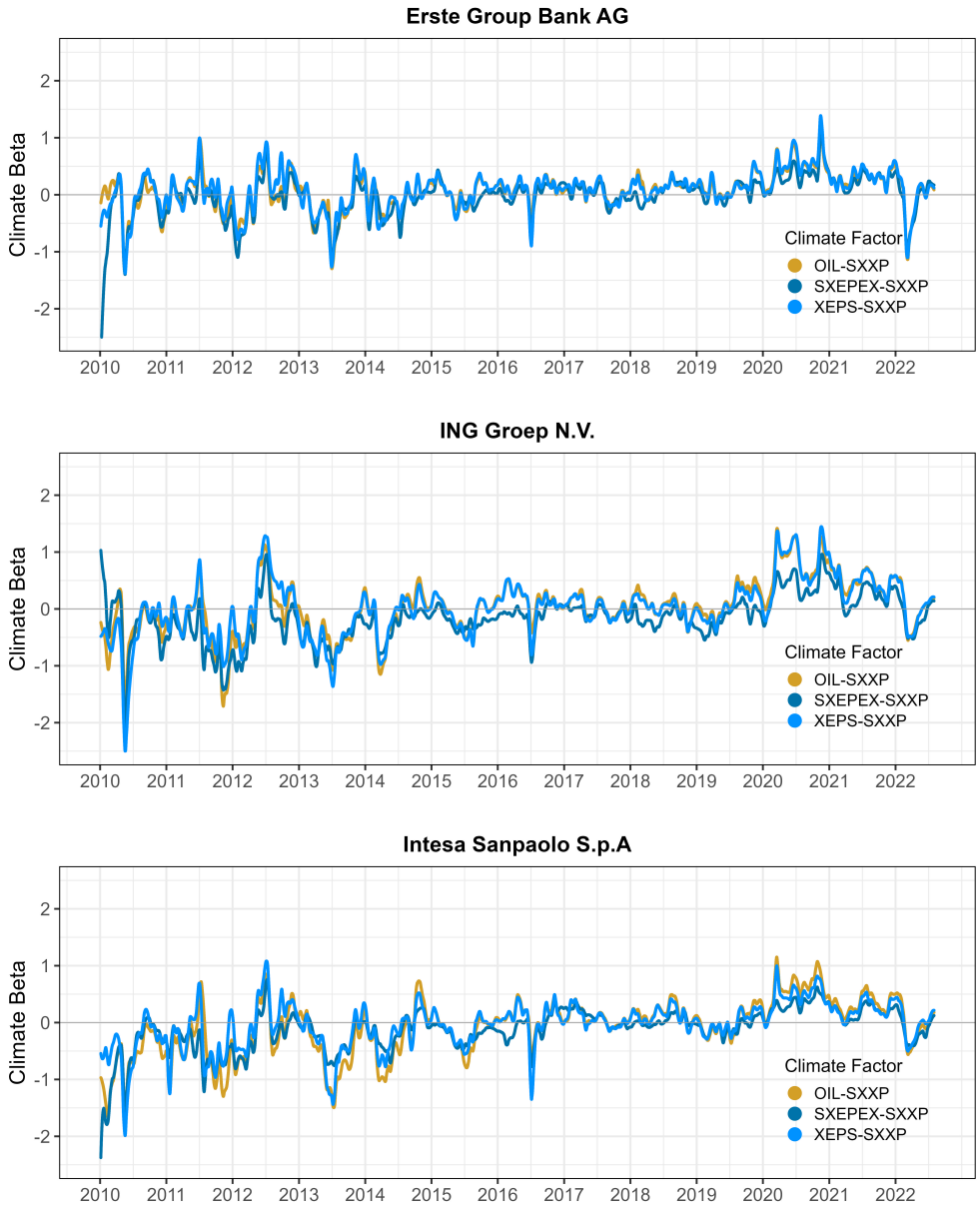

Figure 6: An individual cross-Climate Factor comparison of the MGARCH-t estimated Climate Beta.

F MGARCH-DPM Individual Climate Beta

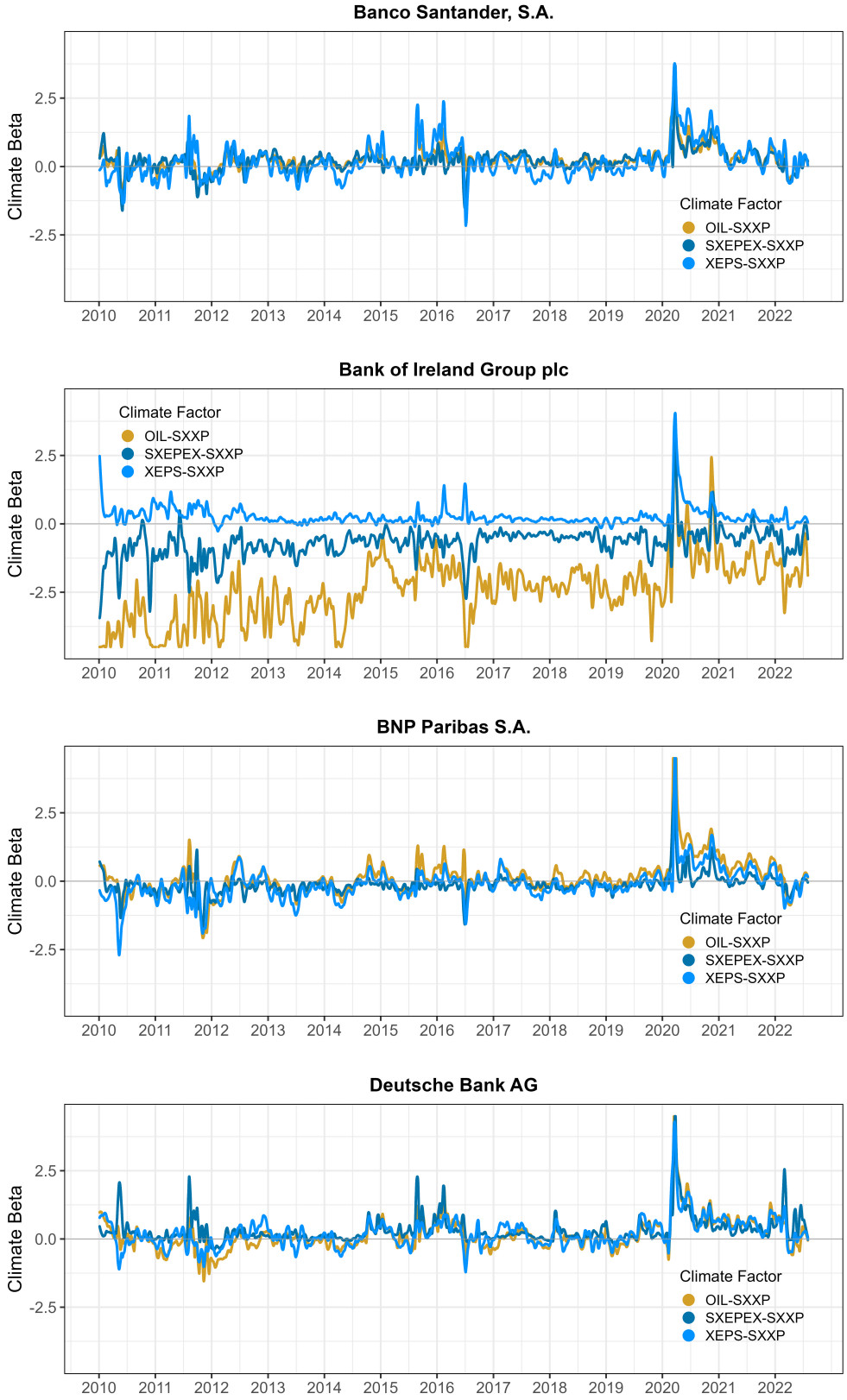

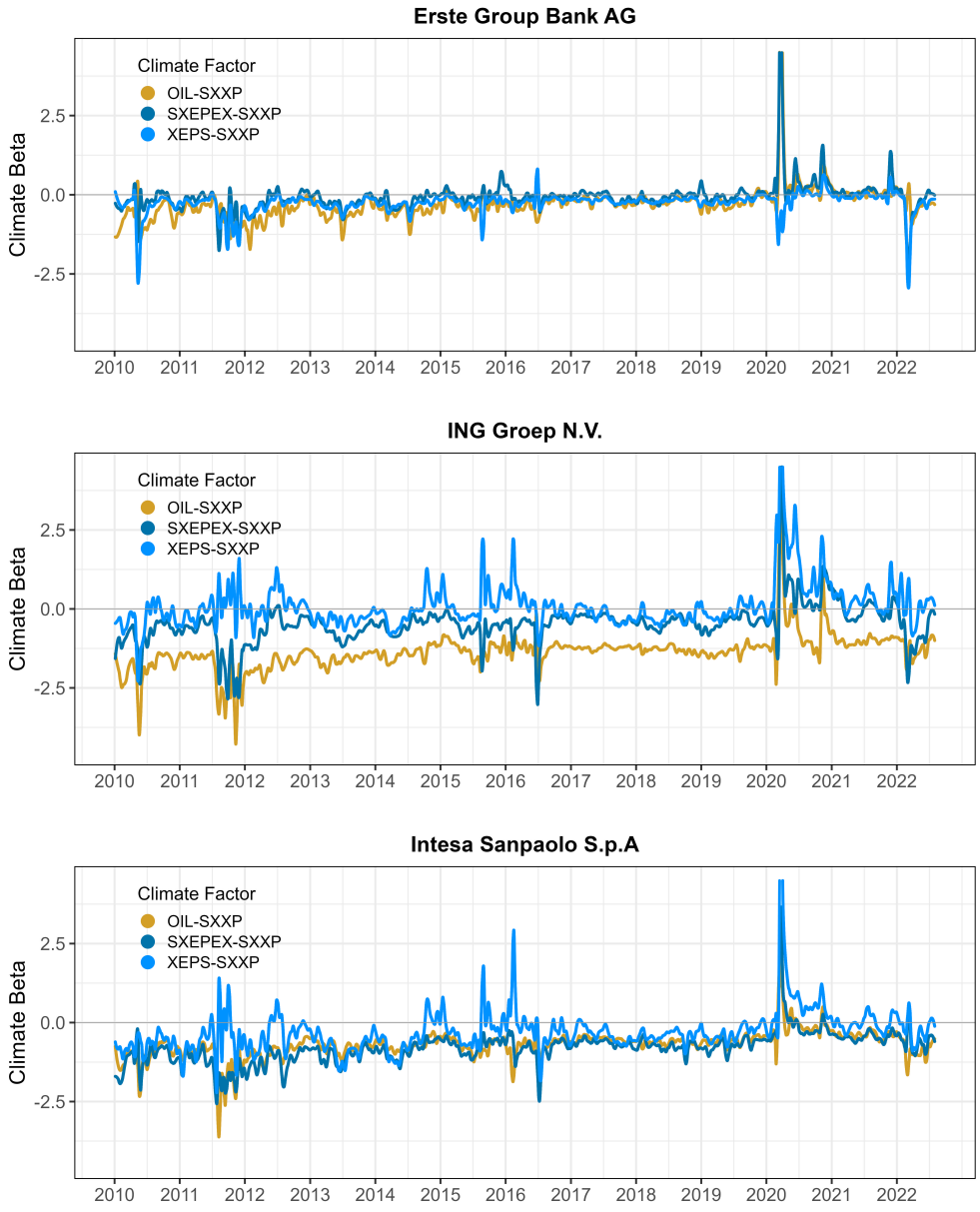

Figure 7: An individual cross-Climate Factor comparison of the MGARCH-DPM estimated Climate Beta conditional on a climate stress severity of $\theta = 0.5$

G MGARCH-t Individual CRISK

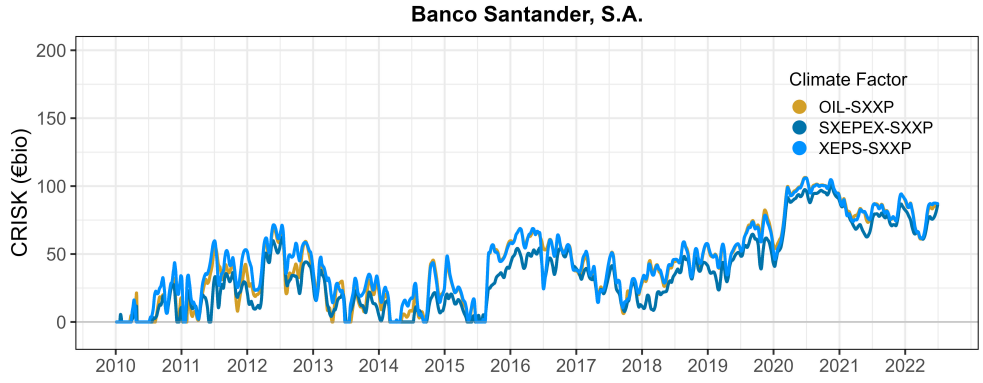

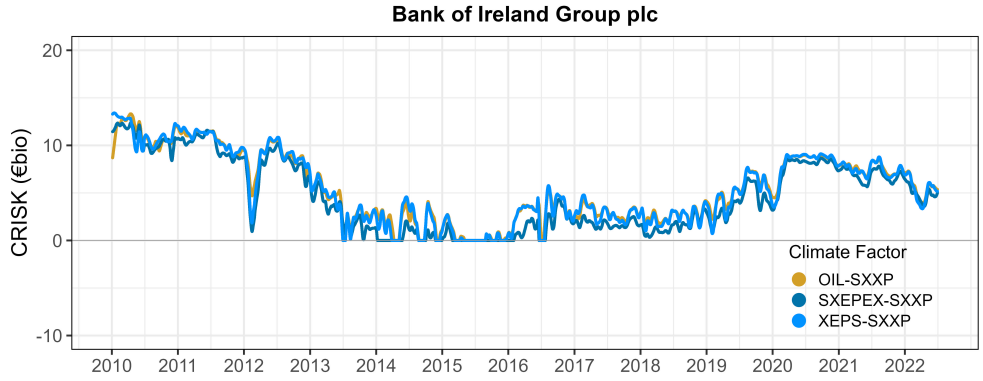

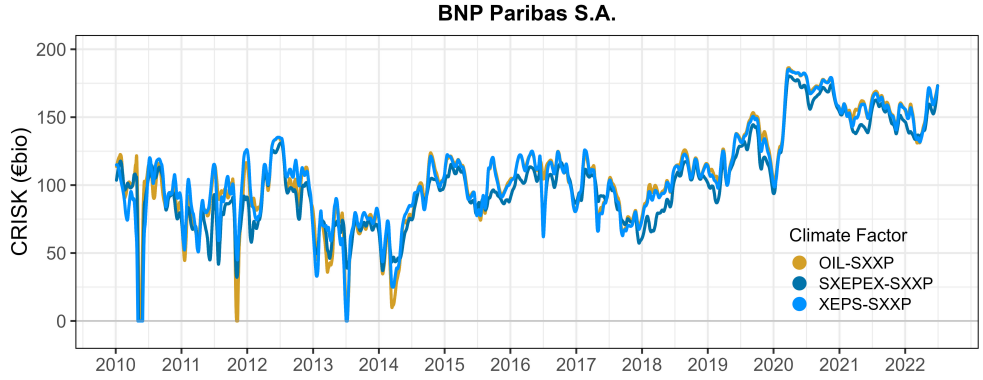

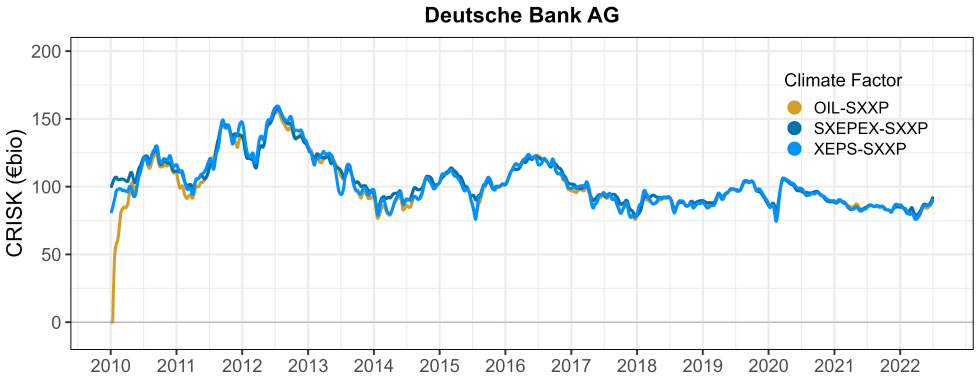

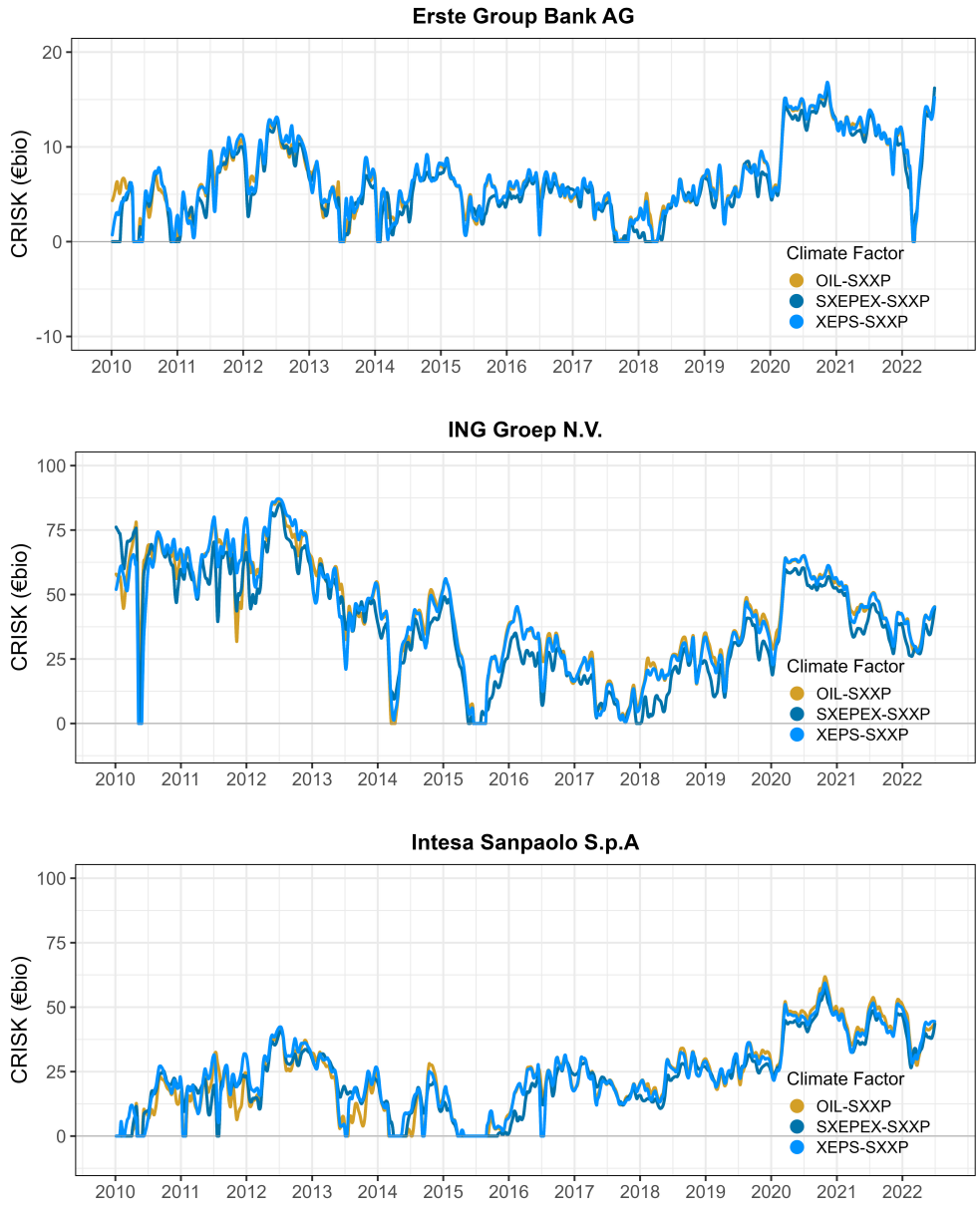

Figure 8: An individual cross-Climate Factor comparison of CRISK applying the MGARCH-t estimated Climate Beta and a climate stress severity of $\theta = 0.5$.

H MGARCH-DPM Individual CRISK

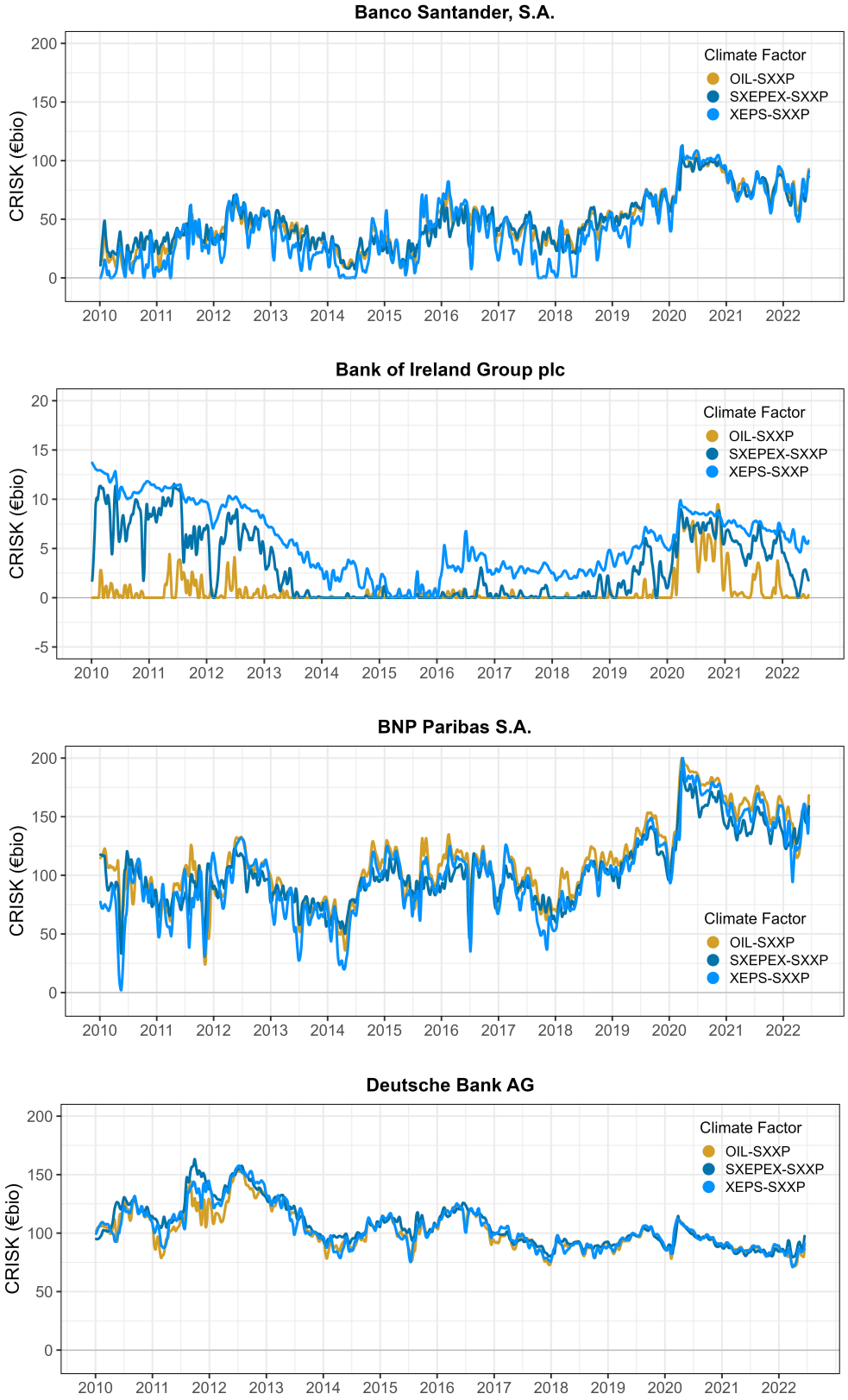

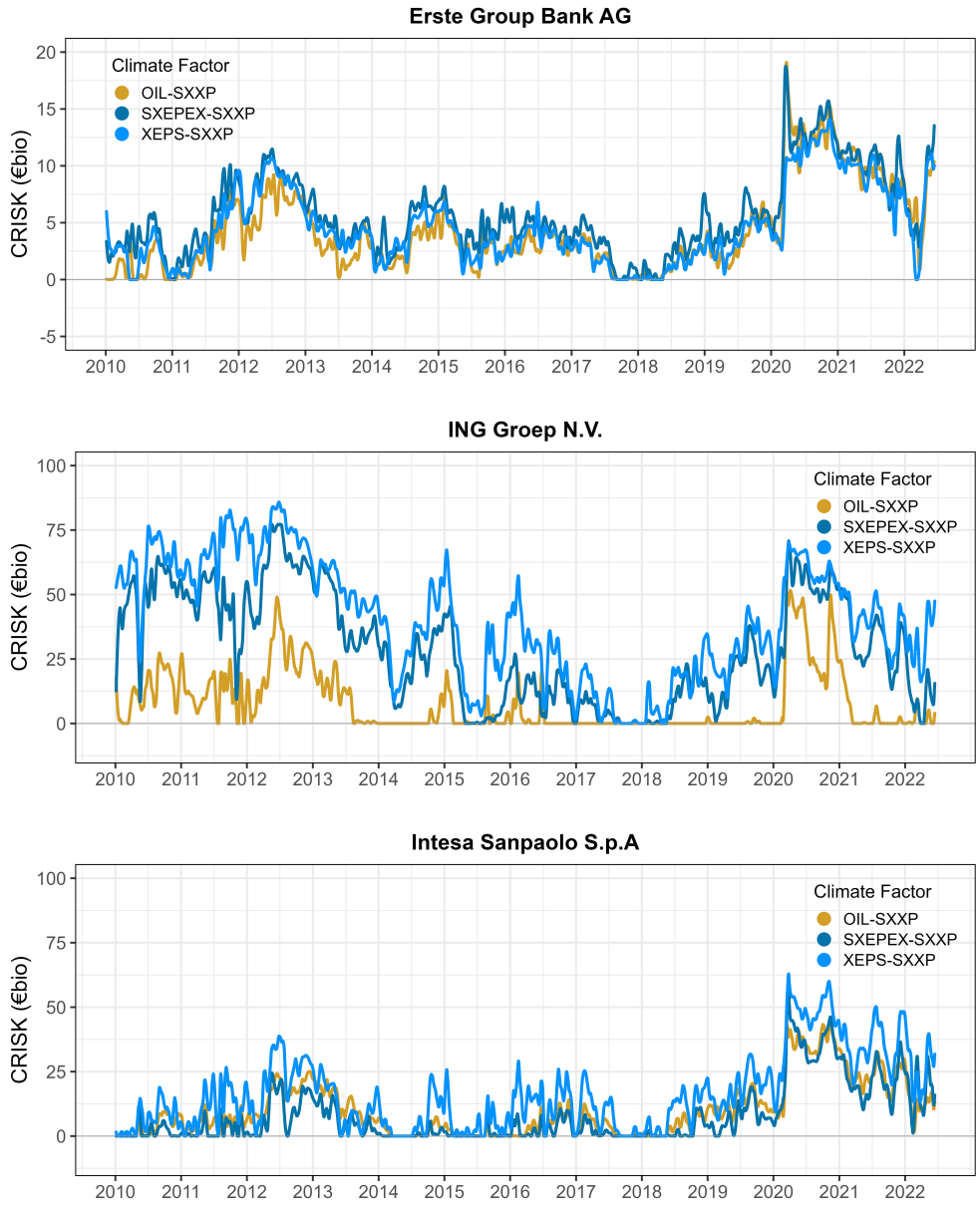

Figure 9: An individual cross-Climate Factor comparison of CRISK applying the MGARCH-DPM estimated Climate Beta conditional on a climate stress severity of $\theta = 0.5$.

I MGARCH-t Combined CRISK

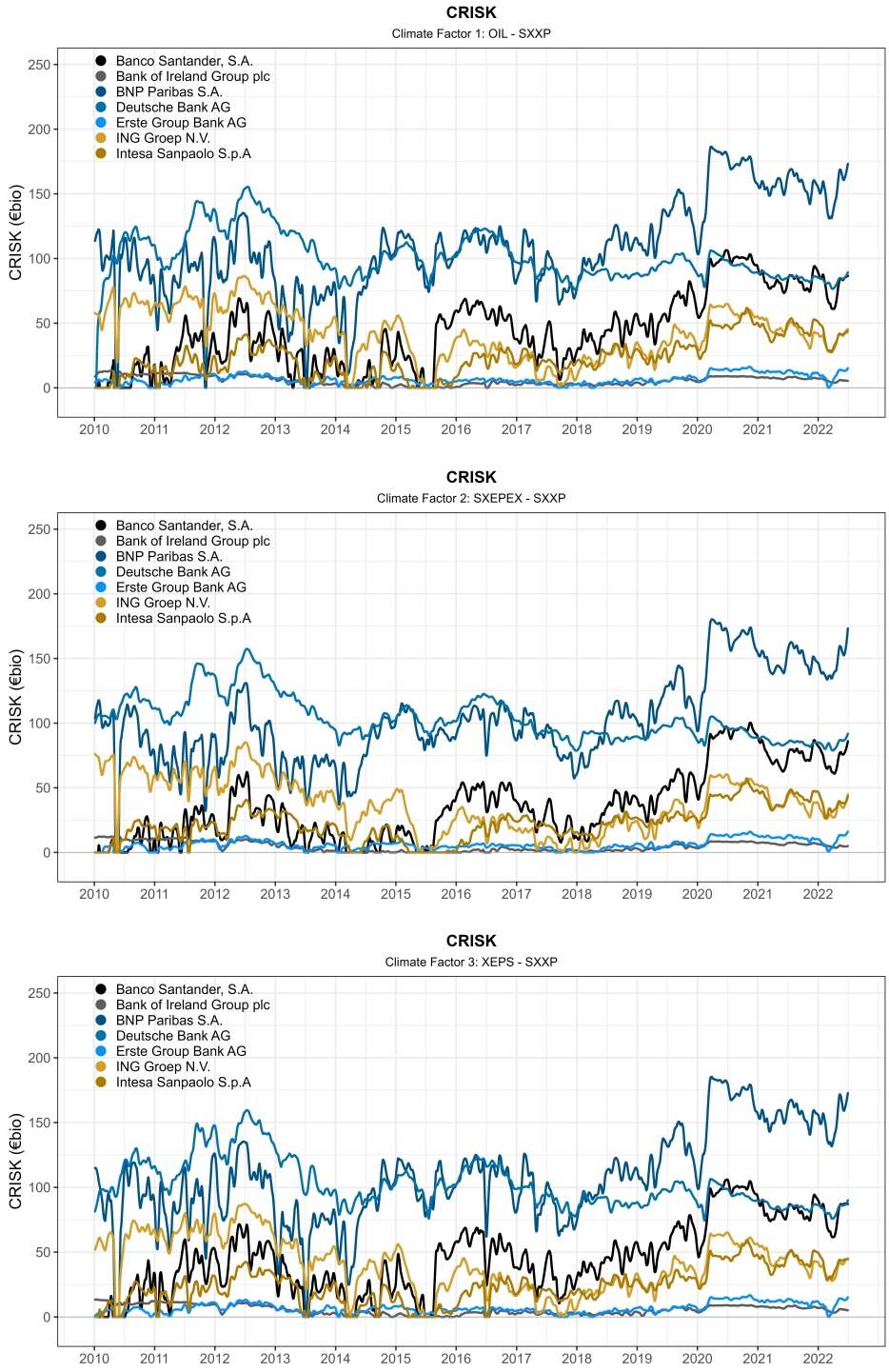

Figure 10: CRISK for all Eurozone banks combined applying a MGARCH-t estimated Climate Beta and a climate stress severity of $\theta = 0.5$. Depicted separately for all Climate Factors.

J MGARCH-DPM Combined CRISK

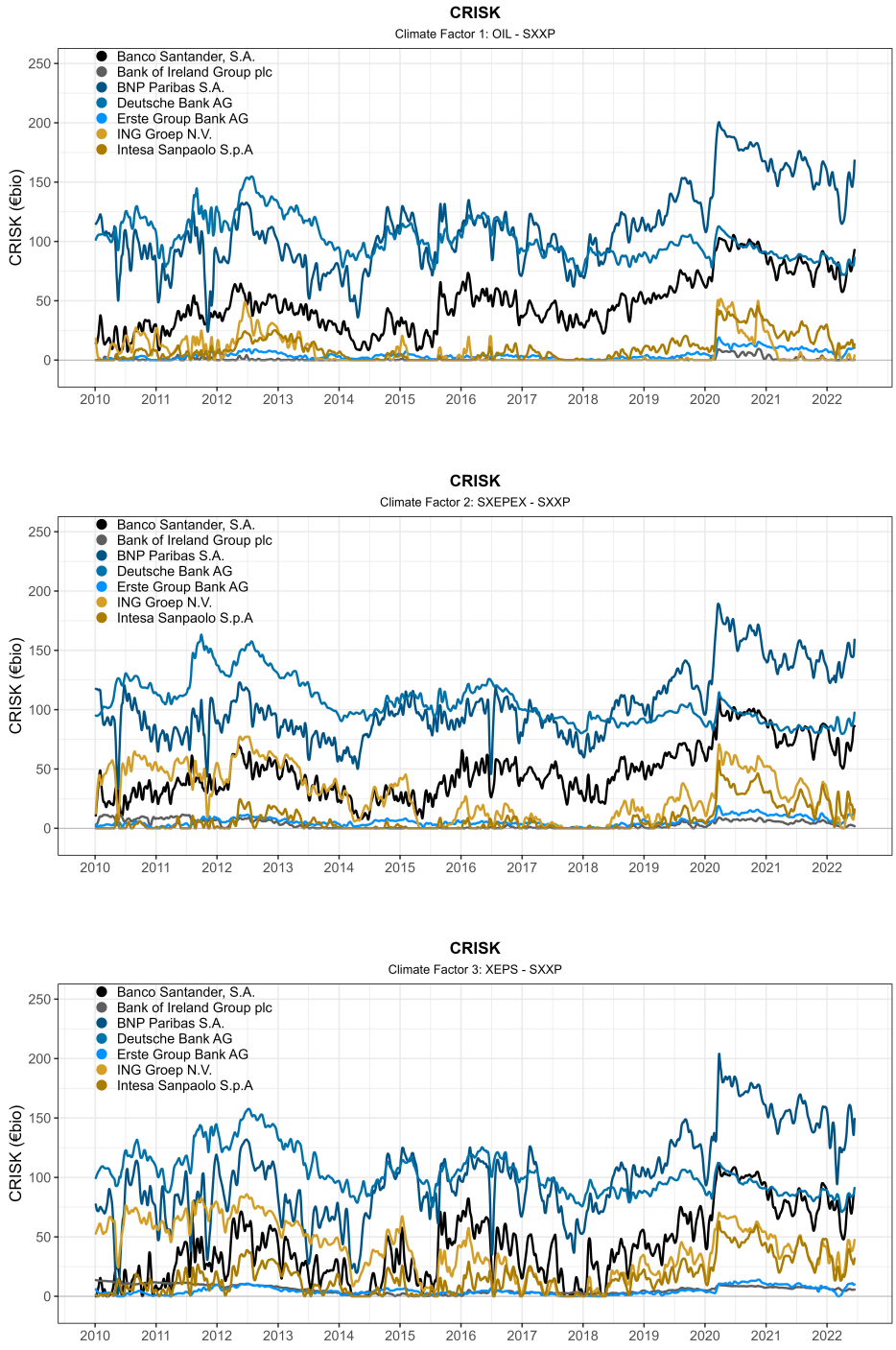

Figure 11: CRISK for all Eurozone banks combined applying a MGARCH-DPM estimated Climate Beta and a climate stress severity of $\theta = 0.5$. Depicted separately for all Climate Factors.

K MGARCH Parameter Estimates

SAN	**MGARCH-t**					
	CF_1		CF_2		CF_3	
	Post. Mean	95% DI	Post. Mean	95% DI	Post. Mean	95% DI
ω_{11}	0.074	(0.047, 0.108)	0.075	(0.049, 0.109)	0.075	(0.049, 0.108)
ω_{22}	0.027	(0.018, 0.036)	0.026	(0.018, 0.036)	0.027	(0.018, 0.037)
ω_{33}	0.007	(0.004, 0.011)	0.013	(0.007, 0.020)	0.009	(0.005, 0.014)
α_{11}	0.050	(0.038, 0.064)	0.050	(0.039, 0.063)	0.051	(0.039, 0.065)
α_{22}	0.083	(0.064, 0.103)	0.078	(0.062, 0.098)	0.084	(0.066, 0.103)
α_{33}	0.046	(0.034, 0.062)	0.054	(0.040, 0.073)	0.060	(0.044, 0.080)
β_{11}	0.904	(0.880, 0.926)	0.904	(0.881, 0.925)	0.903	(0.878, 0.925)
β_{22}	0.847	(0.814, 0.878)	0.852	(0.817, 0.882)	0.846	(0.812, 0.877)
β_{33}	0.922	(0.897, 0.942)	0.906	(0.874, 0.931)	0.900	(0.870, 0.926)
γ	0.023	(0.017, 0.032)	0.021	(0.014, 0.029)	0.024	(0.017, 0.032)
δ	0.953	(0.932, 0.969)	0.953	(0.930, 0.971)	0.947	(0.923, 0.965)
μ_1	0.040	(-0.014, 0.095)	0.039	(-0.015, 0.095)	0.042	(-0.015, 0.100)
μ_2	0.073	(0.049, 0.099)	0.073	(0.049, 0.098)	0.074	(0.048, 0.100)
μ_3	-0.016	(-0.038, 0.006)	-0.030	(-0.056, -0.003)	-0.012	(-0.034, 0.009)
ν	6.472	(5.760, 7.286)	6.436	(5.675, 7.335)	6.665	(5.895, 7.514)
	MGARCH-DPM					
	CF_1		CF_2		CF_3	
	Post. Mean	95% DI	Post. Mean	95% DI	Post. Mean	95% DI
ω_{11}	0.114	(0.056, 0.175)	0.094	(0.040, 0.152)	0.116	(0.059, 0.180)
ω_{22}	0.032	(0.017, 0.049)	0.022	(0.009, 0.036)	0.019	(0.007, 0.035)
ω_{33}	0.038	(0.025, 0.059)	0.047	(0.031, 0.071)	0.046	(0.030, 0.068)
α_{11}	0.032	(0.025, 0.041)	0.037	(0.029, 0.047)	0.036	(0.027, 0.045)
α_{22}	0.043	(0.034, 0.055)	0.052	(0.043, 0.063)	0.046	(0.036, 0.057)
α_{33}	0.031	(0.020, 0.045)	0.047	(0.033, 0.063)	0.092	(0.066, 0.121)
β_{11}	0.911	(0.890, 0.931)	0.915	(0.894, 0.933)	0.905	(0.882, 0.925)
β_{22}	0.847	(0.820, 0.874)	0.864	(0.838, 0.887)	0.868	(0.839, 0.894)
β_{33}	0.878	(0.819, 0.918)	0.880	(0.836, 0.916)	0.838	(0.786, 0.884)
γ	0.014	(0.009, 0.019)	0.015	(0.010, 0.021)	0.026	(0.020, 0.033)
δ	0.897	(0.827, 0.940)	0.948	(0.918, 0.971)	0.934	(0.912, 0.951)

Table 6: Banco Santander, S.A. This table exhibits the posterior mean and 95% density intervals for the parameters of the MGARCH-t and MGARCH-DPM model. The models are fitted on daily return data on SAN SM, the market factor SXXP and one of the 3 Climate Factors: CF_1 OIL - SXXP, CF_2 SXEPEX - SXXP, CF_3 XEPS - SXXP. Data is from 1st of January 2010 to 1st of August 2022.

BIRG	**MGARCH-t**					
	CF_1		CF_2		CF_3	
	Post. Mean	95% DI	Post. Mean	95% DI	Post. Mean	95% DI
ω_{11}	0.079	(0.045, 0.126)	0.075	(0.044, 0.117)	0.082	(0.045, 0.132)
ω_{22}	0.026	(0.018, 0.036)	0.026	(0.017, 0.035)	0.026	(0.018, 0.036)
ω_{33}	0.007	(0.004, 0.011)	0.012	(0.007, 0.019)	0.009	(0.005, 0.014)
α_{11}	0.056	(0.043, 0.071)	0.054	(0.041, 0.070)	0.058	(0.045, 0.077)
α_{22}	0.092	(0.071, 0.115)	0.087	(0.069, 0.108)	0.092	(0.073, 0.112)
α_{33}	0.047	(0.035, 0.062)	0.057	(0.041, 0.076)	0.062	(0.045, 0.083)
β_{11}	0.914	(0.890, 0.934)	0.916	(0.892, 0.936)	0.911	(0.885, 0.931)
β_{22}	0.841	(0.809, 0.873)	0.846	(0.813, 0.876)	0.841	(0.809, 0.871)
β_{33}	0.923	(0.898, 0.943)	0.905	(0.876, 0.930)	0.901	(0.871, 0.926)
γ	0.020	(0.013, 0.029)	0.015	(0.009, 0.023)	0.020	(0.013, 0.027)
δ	0.949	(0.917, 0.969)	0.944	(0.900, 0.971)	0.944	(0.914, 0.965)
μ_1	0.073	(-0.007, 0.150)	0.073	(-0.006, 0.149)	0.070	(-0.010, 0.148)
μ_2	0.069	(0.044, 0.095)	0.068	(0.042, 0.096)	0.069	(0.045, 0.094)
μ_3	-0.012	(-0.034, 0.010)	-0.023	(-0.048, -0.000)	-0.007	(-0.029, 0.015)
ν	7.152	(6.327, 8.128)	7.043	(6.259, 7.914)	7.382	(6.501, 8.415)
	MGARCH-DPM					
	CF_1		CF_2		CF_3	
	Post. Mean	95% DI	Post. Mean	95% DI	Post. Mean	95% DI
ω_{11}	0.159	(0.104, 0.220)	0.111	(0.054, 0.171)	0.144	(0.090, 0.203)
ω_{22}	0.014	(0.006, 0.025)	0.018	(0.008, 0.028)	0.015	(0.007, 0.029)
ω_{33}	0.036	(0.025, 0.054)	0.034	(0.020, 0.050)	0.022	(0.015, 0.033)
α_{11}	0.054	(0.043, 0.065)	0.038	(0.027, 0.051)	0.057	(0.045, 0.073)
α_{22}	0.076	(0.063, 0.091)	0.075	(0.059, 0.089)	0.058	(0.044, 0.073)
α_{33}	0.034	(0.023, 0.050)	0.061	(0.043, 0.084)	0.047	(0.033, 0.066)
β_{11}	0.921	(0.906, 0.935)	0.945	(0.930, 0.959)	0.926	(0.908, 0.943)
β_{22}	0.842	(0.817, 0.864)	0.835	(0.805, 0.865)	0.857	(0.824, 0.886)
β_{33}	0.888	(0.841, 0.920)	0.884	(0.842, 0.921)	0.899	(0.859, 0.928)
γ	0.012	(0.005, 0.020)	0.009	(0.004, 0.014)	0.008	(0.004, 0.014)
δ	0.851	(0.584, 0.955)	0.822	(0.511, 0.932)	0.900	(0.708, 0.965)

Table 7: Bank of Ireland Group plc. This table exhibits the posterior mean and 95% density intervals for the parameters of the MGARCH-t and MGARCH-DPM model. The models are fitted on daily return data on BIRG LON, the market factor SXXP and one of the 3 Climate Factors: CF_1 OIL - SXXP, CF_2 SXEPEX - SXXP, CF_3 XEPS - SXXP. Data is from 1st of January 2010 to 1st of August 2022.

BNP			**MGARCH-t**			
	CF_1		CF_2		CF_3	
	Post. Mean	95% DI	Post. Mean	95% DI	Post. Mean	95% DI
ω_{11}	0.059	(0.038, 0.086)	0.057	(0.037, 0.083)	0.062	(0.042, 0.088)
ω_{22}	0.024	(0.016, 0.033)	0.024	(0.016, 0.033)	0.025	(0.018, 0.034)
ω_{33}	0.006	(0.003, 0.010)	0.011	(0.006, 0.017)	0.008	(0.005, 0.014)
α_{11}	0.055	(0.043, 0.069)	0.054	(0.042, 0.067)	0.057	(0.045, 0.070)
α_{22}	0.072	(0.056, 0.091)	0.070	(0.053, 0.089)	0.076	(0.060, 0.095)
α_{33}	0.046	(0.035, 0.060)	0.051	(0.037, 0.068)	0.062	(0.046, 0.081)
β_{11}	0.904	(0.881, 0.923)	0.906	(0.884, 0.926)	0.901	(0.880, 0.920)
β_{22}	0.865	(0.834, 0.894)	0.867	(0.834, 0.896)	0.859	(0.828, 0.888)
β_{33}	0.925	(0.903, 0.943)	0.913	(0.886, 0.936)	0.901	(0.870, 0.927)
γ	0.028	(0.020, 0.036)	0.022	(0.015, 0.031)	0.030	(0.021, 0.038)
δ	0.947	(0.924, 0.964)	0.950	(0.923, 0.969)	0.937	(0.911, 0.957)
μ_1	0.060	(0.010, 0.113)	0.058	(0.005, 0.114)	0.061	(0.008, 0.113)
μ_2	0.065	(0.040, 0.089)	0.064	(0.039, 0.090)	0.066	(0.040, 0.090)
μ_3	-0.018	(-0.039, 0.003)	-0.029	(-0.055, -0.005)	-0.014	(-0.037, 0.009)
ν	6.888	(6.076, 7.866)	6.735	(5.915, 7.690)	7.045	(6.190, 8.036)
			MGARCH-DPM			
	CF_1		CF_2		CF_3	
	Post. Mean	95% DI	Post. Mean	95% DI	Post. Mean	95% DI
ω_{11}	0.124	(0.083, 0.173)	0.184	(0.123, 0.260)	0.118	(0.068, 0.175)
ω_{22}	0.019	(0.009, 0.036)	0.029	(0.014, 0.050)	0.024	(0.011, 0.040)
ω_{33}	0.029	(0.019, 0.045)	0.064	(0.041, 0.094)	0.030	(0.020, 0.043)
α_{11}	0.046	(0.037, 0.055)	0.034	(0.025, 0.046)	0.058	(0.046, 0.073)
α_{22}	0.056	(0.046, 0.069)	0.039	(0.030, 0.050)	0.064	(0.051, 0.080)
α_{33}	0.049	(0.034, 0.070)	0.041	(0.027, 0.056)	0.086	(0.064, 0.114)
β_{11}	0.901	(0.880, 0.918)	0.884	(0.853, 0.909)	0.889	(0.864, 0.909)
β_{22}	0.860	(0.838, 0.882)	0.853	(0.816, 0.880)	0.848	(0.817, 0.874)
β_{33}	0.891	(0.845, 0.923)	0.856	(0.800, 0.900)	0.866	(0.821, 0.900)
γ	0.016	(0.013, 0.021)	0.014	(0.009, 0.020)	0.025	(0.017, 0.032)
δ	0.959	(0.943, 0.972)	0.929	(0.882, 0.961)	0.929	(0.901, 0.952)

Table 8: BNP Paribas S.A. This table exhibits the posterior mean and 95% density intervals for the parameters of the MGARCH-t and MGARCH-DPM model. The models are fitted on daily return data on BNP FP, the market factor SXXP and one of the 3 Climate Factors: CF_1 OIL - SXXP, CF_2 SXEPEX - SXXP, CF_3 XEPS - SXXP. Data is from 1st of January 2010 to 1st of August 2022.

DBK			**MGARCH-t**			
	CF_1		CF_2		CF_3	
	Post. Mean	95% DI	Post. Mean	95% DI	Post. Mean	95% DI
ω_{11}	0.081	(0.048, 0.124)	0.073	(0.043, 0.114)	0.081	(0.048, 0.128)
ω_{22}	0.028	(0.020, 0.038)	0.027	(0.019, 0.038)	0.028	(0.019, 0.038)
ω_{33}	0.006	(0.003, 0.010)	0.011	(0.007, 0.018)	0.009	(0.005, 0.013)
α_{11}	0.041	(0.029, 0.055)	0.038	(0.028, 0.051)	0.041	(0.030, 0.056)
α_{22}	0.088	(0.067, 0.108)	0.083	(0.064, 0.104)	0.089	(0.069, 0.111)
α_{33}	0.043	(0.031, 0.058)	0.049	(0.036, 0.068)	0.057	(0.042, 0.077)
β_{11}	0.917	(0.890, 0.941)	0.924	(0.897, 0.943)	0.918	(0.889, 0.940)
β_{22}	0.837	(0.803, 0.870)	0.843	(0.807, 0.875)	0.837	(0.801, 0.869)
β_{33}	0.927	(0.903, 0.947)	0.912	(0.882, 0.935)	0.905	(0.876, 0.931)
γ	0.015	(0.009, 0.022)	0.016	(0.009, 0.024)	0.016	(0.010, 0.024)
δ	0.970	(0.950, 0.983)	0.962	(0.934, 0.984)	0.963	(0.938, 0.980)
μ_1	0.030	(-0.032, 0.091)	0.031	(-0.025, 0.092)	0.033	(-0.030, 0.094)
μ_2	0.073	(0.049, 0.099)	0.073	(0.050, 0.098)	0.073	(0.049, 0.099)
μ_3	-0.014	(-0.037, 0.008)	-0.026	(-0.051, 0.000)	-0.011	(-0.033, 0.012)
ν	6.188	(5.488, 6.943)	6.100	(5.457, 6.813)	6.388	(5.711, 7.164)
			MGARCH-DPM			
	CF_1		CF_2		CF_3	
	Post. Mean	95% DI	Post. Mean	95% DI	Post. Mean	95% DI
ω_{11}	0.256	(0.166, 0.416)	0.219	(0.116, 0.332)	0.206	(0.137, 0.324)
ω_{22}	0.041	(0.020, 0.068)	0.034	(0.013, 0.059)	0.031	(0.014, 0.050)
ω_{33}	0.018	(0.012, 0.029)	0.043	(0.029, 0.060)	0.037	(0.025, 0.051)
α_{11}	0.030	(0.021, 0.043)	0.027	(0.018, 0.038)	0.030	(0.021, 0.041)
α_{22}	0.045	(0.035, 0.057)	0.051	(0.040, 0.066)	0.067	(0.052, 0.084)
α_{33}	0.016	(0.011, 0.024)	0.033	(0.024, 0.044)	0.066	(0.049, 0.090)
β_{11}	0.900	(0.855, 0.928)	0.906	(0.869, 0.937)	0.918	(0.880, 0.942)
β_{22}	0.832	(0.791, 0.866)	0.824	(0.784, 0.860)	0.831	(0.792, 0.862)
β_{33}	0.934	(0.903, 0.955)	0.872	(0.832, 0.908)	0.864	(0.815, 0.901)
γ	0.006	(0.003, 0.008)	0.006	(0.001, 0.011)	0.014	(0.009, 0.019)
δ	0.965	(0.938, 0.981)	0.926	(0.839, 0.999)	0.956	(0.935, 0.974)

Table 9: Deutsche Bank AG. This table exhibits the posterior mean and 95% density intervals for the parameters of the MGARCH-t and MGARCH-DPM model. The models are fitted on daily return data on DBK GR, the market factor SXXP and one of the 3 Climate Factors: CF_1 OIL - SXXP, CF_2 SXEPEX - SXXP, CF_3 XEPS - SXXP. Data is from 1st of January 2010 to 1st of August 2022.

EBS			**MGARCH-t**			
	CF_1		CF_2		CF_3	
	Post. Mean	95% DI	Post. Mean	95% DI	Post. Mean	95% DI
ω_{11}	0.115	(0.076, 0.169)	0.117	(0.074, 0.170)	0.116	(0.076, 0.163)
ω_{22}	0.030	(0.021, 0.041)	0.031	(0.021, 0.042)	0.031	(0.022, 0.041)
ω_{33}	0.006	(0.004, 0.010)	0.012	(0.007, 0.019)	0.009	(0.005, 0.014)
α_{11}	0.059	(0.045, 0.076)	0.061	(0.046, 0.078)	0.059	(0.046, 0.076)
α_{22}	0.091	(0.072, 0.114)	0.090	(0.069, 0.112)	0.092	(0.072, 0.115)
α_{33}	0.046	(0.034, 0.062)	0.055	(0.039, 0.075)	0.061	(0.044, 0.082)
β_{11}	0.881	(0.849, 0.907)	0.878	(0.845, 0.907)	0.881	(0.850, 0.909)
β_{22}	0.831	(0.796, 0.865)	0.831	(0.795, 0.868)	0.831	(0.793, 0.862)
β_{33}	0.924	(0.901, 0.943)	0.907	(0.875, 0.931)	0.901	(0.868, 0.927)
γ	0.022	(0.015, 0.031)	0.021	(0.013, 0.030)	0.023	(0.016, 0.032)
δ	0.942	(0.913, 0.964)	0.932	(0.887, 0.961)	0.935	(0.906, 0.958)
μ_1	0.096	(0.040, 0.153)	0.094	(0.036, 0.156)	0.097	(0.037, 0.153)
μ_2	0.070	(0.043, 0.096)	0.070	(0.043, 0.097)	0.070	(0.045, 0.095)
μ_3	-0.014	(-0.037, 0.009)	-0.025	(-0.052, -0.000)	-0.010	(-0.033, 0.013)
ν	6.762	(6.002, 7.640)	6.803	(6.092, 7.717)	6.940	(6.156, 7.884)
			MGARCH-DPM			
	CF_1		CF_2		CF_3	
	Post. Mean	95% DI	Post. Mean	95% DI	Post. Mean	95% DI
ω_{11}	0.242	(0.153, 0.375)	0.294	(0.197, 0.428)	0.204	(0.129, 0.303)
ω_{22}	0.020	(0.010, 0.038)	0.026	(0.009, 0.044)	0.019	(0.006, 0.036)
ω_{33}	0.025	(0.016, 0.035)	0.039	(0.025, 0.062)	0.052	(0.031, 0.075)
α_{11}	0.057	(0.041, 0.077)	0.046	(0.035, 0.060)	0.064	(0.048, 0.082)
α_{22}	0.061	(0.048, 0.076)	0.043	(0.034, 0.056)	0.054	(0.041, 0.066)
α_{33}	0.029	(0.021, 0.038)	0.029	(0.019, 0.042)	0.058	(0.038, 0.082)
β_{11}	0.882	(0.847, 0.913)	0.862	(0.822, 0.895)	0.881	(0.845, 0.910)
β_{22}	0.852	(0.821, 0.878)	0.853	(0.823, 0.878)	0.853	(0.823, 0.884)
β_{33}	0.914	(0.884, 0.940)	0.894	(0.842, 0.931)	0.862	(0.805, 0.912)
γ	0.014	(0.010, 0.019)	0.012	(0.007, 0.017)	0.015	(0.009, 0.022)
δ	0.946	(0.921, 0.966)	0.915	(0.852, 0.954)	0.917	(0.851, 0.958)

Table 10: Erste Group Bank AG. This table exhibits the posterior mean and 95% density intervals for the parameters of the MGARCH-t and MGARCH-DPM model. The models are fitted on daily return data on EBS AV, the market factor SXXP and one of the 3 Climate Factors: CF_1 OIL - SXXP, CF_2 SXEPEX - SXXP, CF_3 XEPS - SXXP. Data is from 1st of January 2010 to 1st of August 2022.

ING			**MGARCH-t**			
	CF_1		CF_2		CF_3	
	Post. Mean	95% DI	Post. Mean	95% DI	Post. Mean	95% DI
ω_{11}	0.056	(0.036, 0.082)	0.056	(0.035, 0.083)	0.056	(0.036, 0.082)
ω_{22}	0.023	(0.016, 0.032)	0.023	(0.016, 0.032)	0.024	(0.017, 0.033)
ω_{33}	0.006	(0.003, 0.010)	0.011	(0.006, 0.018)	0.008	(0.005, 0.013)
α_{11}	0.053	(0.041, 0.067)	0.053	(0.041, 0.066)	0.053	(0.042, 0.065)
α_{22}	0.071	(0.054, 0.089)	0.069	(0.054, 0.086)	0.072	(0.056, 0.091)
α_{33}	0.044	(0.032, 0.058)	0.052	(0.038, 0.070)	0.056	(0.042, 0.077)
β_{11}	0.902	(0.878, 0.922)	0.903	(0.877, 0.924)	0.903	(0.881, 0.922)
β_{22}	0.862	(0.828, 0.892)	0.864	(0.831, 0.892)	0.861	(0.829, 0.889)
β_{33}	0.925	(0.901, 0.945)	0.910	(0.880, 0.932)	0.906	(0.873, 0.929)
γ	0.024	(0.017, 0.031)	0.020	(0.014, 0.027)	0.025	(0.018, 0.033)
δ	0.954	(0.936, 0.969)	0.959	(0.939, 0.974)	0.950	(0.929, 0.966)
μ_1	0.072	(0.021, 0.123)	0.073	(0.019, 0.125)	0.073	(0.018, 0.129)
μ_2	0.066	(0.041, 0.090)	0.066	(0.041, 0.091)	0.067	(0.043, 0.092)
μ_3	-0.015	(-0.037, 0.008)	-0.028	(-0.051, -0.004)	-0.010	(-0.031, 0.012)
ν	5.814	(5.250, 6.459)	5.932	(5.315, 6.675)	6.003	(5.351, 6.737)
			MGARCH-DPM			
	CF_1		CF_2		CF_3	
	Post. Mean	95% DI	Post. Mean	95% DI	Post. Mean	95% DI
ω_{11}	0.166	(0.118, 0.235)	0.167	(0.105, 0.247)	0.193	(0.133, 0.269)
ω_{22}	0.029	(0.016, 0.046)	0.040	(0.023, 0.058)	0.044	(0.026, 0.064)
ω_{33}	0.014	(0.010, 0.021)	0.054	(0.033, 0.078)	0.033	(0.021, 0.053)
α_{11}	0.043	(0.035, 0.053)	0.046	(0.035, 0.059)	0.050	(0.040, 0.062)
α_{22}	0.052	(0.042, 0.065)	0.052	(0.041, 0.066)	0.054	(0.043, 0.067)
α_{33}	0.033	(0.026, 0.045)	0.066	(0.047, 0.091)	0.064	(0.044, 0.088)
β_{11}	0.894	(0.869, 0.912)	0.895	(0.870, 0.918)	0.888	(0.859, 0.911)
β_{22}	0.858	(0.835, 0.884)	0.853	(0.823, 0.882)	0.847	(0.812, 0.874)
β_{33}	0.939	(0.919, 0.953)	0.831	(0.775, 0.881)	0.877	(0.829, 0.917)
γ	0.017	(0.012, 0.022)	0.013	(0.008, 0.018)	0.016	(0.010, 0.023)
δ	0.947	(0.927, 0.963)	0.935	(0.897, 0.964)	0.945	(0.906, 0.967)

Table 11: ING Groep N.V. This table exhibits the posterior mean and 95% density intervals for the parameters of the MGARCH-t and MGARCH-DPM model. The models are fitted on daily return data on ING NA, the market factor SXXP and one of the 3 Climate Factors: CF_1 OIL - SXXP, CF_2 SXEPEX - SXXP, CF_3 XEPS - SXXP. Data is from 1st of January 2010 to 1st of August 2022.

ISP			**MGARCH-t**			
	CF_1		CF_2		CF_3	
	Post. Mean	95% DI	Post. Mean	95% DI	Post. Mean	95% DI
ω_{11}	0.050	(0.030, 0.074)	0.052	(0.032, 0.076)	0.050	(0.030, 0.075)
ω_{22}	0.021	(0.014, 0.030)	0.022	(0.015, 0.031)	0.021	(0.014, 0.030)
ω_{33}	0.006	(0.003, 0.010)	0.011	(0.007, 0.017)	0.009	(0.005, 0.013)
α_{11}	0.067	(0.052, 0.084)	0.066	(0.051, 0.081)	0.067	(0.053, 0.083)
α_{22}	0.075	(0.058, 0.094)	0.074	(0.057, 0.093)	0.077	(0.058, 0.097)
α_{33}	0.046	(0.034, 0.062)	0.054	(0.039, 0.072)	0.062	(0.046, 0.081)
β_{11}	0.894	(0.870, 0.915)	0.895	(0.874, 0.916)	0.894	(0.870, 0.915)
β_{22}	0.866	(0.832, 0.896)	0.866	(0.833, 0.893)	0.863	(0.831, 0.893)
β_{33}	0.924	(0.898, 0.944)	0.909	(0.881, 0.932)	0.900	(0.869, 0.925)
γ	0.020	(0.014, 0.027)	0.019	(0.013, 0.026)	0.020	(0.014, 0.027)
δ	0.961	(0.945, 0.973)	0.958	(0.941, 0.972)	0.960	(0.943, 0.973)
μ_1	0.096	(0.039, 0.149)	0.096	(0.040, 0.151)	0.096	(0.041, 0.153)
μ_2	0.075	(0.050, 0.099)	0.074	(0.048, 0.098)	0.074	(0.048, 0.099)
μ_3	-0.016	(-0.039, 0.006)	-0.030	(-0.055, -0.005)	-0.011	(-0.032, 0.011)
ν	6.454	(5.710, 7.282)	6.506	(5.733, 7.419)	6.621	(5.850, 7.482)
			MGARCH-DPM			
	CF_1		CF_2		CF_3	
	Post. Mean	95% DI	Post. Mean	95% DI	Post. Mean	95% DI
ω_{11}	0.232	(0.152, 0.332)	0.179	(0.119, 0.260)	0.204	(0.133, 0.274)
ω_{22}	0.029	(0.012, 0.048)	0.021	(0.009, 0.034)	0.021	(0.009, 0.037)
ω_{33}	0.049	(0.031, 0.077)	0.067	(0.046, 0.097)	0.038	(0.026, 0.054)
α_{11}	0.045	(0.034, 0.058)	0.044	(0.033, 0.055)	0.045	(0.034, 0.057)
α_{22}	0.044	(0.032, 0.058)	0.044	(0.034, 0.053)	0.037	(0.030, 0.046)
α_{33}	0.036	(0.024, 0.056)	0.044	(0.030, 0.060)	0.061	(0.045, 0.081)
β_{11}	0.876	(0.842, 0.904)	0.882	(0.855, 0.908)	0.876	(0.850, 0.903)
β_{22}	0.862	(0.826, 0.896)	0.868	(0.841, 0.893)	0.872	(0.841, 0.897)
β_{33}	0.840	(0.757, 0.896)	0.806	(0.730, 0.866)	0.875	(0.831, 0.909)
γ	0.009	(0.006, 0.013)	0.008	(0.005, 0.012)	0.012	(0.008, 0.016)
δ	0.951	(0.920, 0.970)	0.948	(0.901, 0.972)	0.943	(0.915, 0.961)

Table 12: Intesa Sanpaolo S.p.A. This table exhibits the posterior mean and 95% density intervals for the parameters of the MGARCH-t and MGARCH-DPM model. The models are fitted on daily return data on ISP IM, the market factor SXXP and one of the 3 Climate Factors: CF_1 OIL - SXXP, CF_2 SXEPEX - SXXP, CF_3 XEPS - SXXP. Data is from 1st of January 2010 to 1st of August 2022.

L Summary of Programming Files

Below we outline the programming files used for the empirical study. All files are coded in RStudio, except for the MGARCH-DPM model code which is partly coded in C++.

Folder bmgarch-master

The folder `bmgarch-master` consists of the adjusted `bmgarch` package (Rast & Martin, 2021). The functions below are adjusted for our analysis.

- `bmgarch.R`
  Function that calls the stan model to fit the MGARCH parameters. For the MGARCH-t model select 'student-t'. For the MGARCH-DPM model select 'gaussian_dpm'.
- `DCCMGARCH.stan`
  Estimates the MGARCH process with DCC parametrization for both the MGARCH-t and MGARCH-DPM model.

Folder main code

This folder contains all the main code to run our empirical study.

- `main_bmgarch.r`
  Estimates the MGARCH process with DCC parametrization for the benchmark MGARCH-t model as outlined in Section 3.2.
- `main_bmgarchdpm.r`
  Estimates the MGARCH process with DCC parametrization and Dirichlet mixture over the mean and conditional covariance for our MGARCH-DPM model as outlined in Section 3.3. The main file contains the following functions which work together with the `dirichletprocess` package (Ross & Markwick, 2022).
  - `ClusterParameterUpdateGARCH`
  - `Likelihood.mvnormal_garch`
  - `PriorDraw.mvnormal_garch`
  - `PosteriorDraw.mvnormal_garch`
  - `MvnormalGARCHCreate`
  - `InitialiseGARCH`
  - `FitGARCH`
- `main_bmgarchdataprocessing.r`
  Processes the MGARCH-t estimates to compute the Climate Beta and CRISK.
- `main_bmgarchdpmdataprocessing.r`
  Processes the MGARCH-DPM estimates to compute the Climate Beta and CRISK.
- `main_nonparametricbeta.r`
  Computes the non-parametric dynamic conditional Climate Beta according to Section 3.3.4.